

EXPERIMENTAL ANALYSIS OF THE FATIGUE BEHAVIOR OF RECYCLED HIGH-
DENSITY POLYETHYLENE GLASS FIBER COMPOSITES

A Thesis

by

HANNAH ELIZABETH TOERNER

Submitted to the Office of Graduate and Professional Studies of
Texas A&M University
in partial fulfillment of the requirements for the degree of

MASTER OF SCIENCE

Chair of Committee,	David Allen
Committee Members,	Robert Randall
	Vinayak Krishnamurthy
Head of Department,	Sharath Girimaji

May 2020

Major Subject: Ocean Engineering

Copyright 2020 Hannah Toerner

ABSTRACT

This research focuses on the analysis of the mechanical responses of a recycled high-density polyethylene glass fiber composite material when subjected to uniaxial tension fatigue. The desired properties were determined through experimental testing of specimens extracted from crossties composed of the aforementioned material. Results and data gathered from the experiment were compared to the properties of material currently used in fields that provide potential use for the polymer composite. Following the experimental analysis, a computational finite element model was constructed to study the effects of gripping on the mechanical response of the specimens. A further detailed analysis was performed to study the effects of surface pores on specimen performance. Upon completing the experiments and computational finite element analysis, recommendations for improvement in the material were made, and a detailed procedure to be used in conducting further experimental research was established.

DEDICATION

This thesis is dedicated to my parents, Edward and Theresa Toerner. Without their guidance, encouragement, and constant support my undergraduate and graduate work would not be possible.

ACKNOWLEDGEMENTS

I would like to acknowledge Dr. Allen for ensuring that I had the means and resources available to complete this project.

Funding for this research was provided by Axion Structural Innovations, which made this research possible.

I would like to thank my committee members, Dr. Randall for serving as a mentor and support system throughout my undergraduate and graduate career. Dr. Krishnamurthy made one of my weakest subjects an enjoyable course, which taught me the skills I needed to carry out proper analysis.

The staff out at RELLIS, particularly Dr. Keating and Charlie Droddy, and their advice and insights were immensely important to the completion of this project.

Thank you to my friends and colleagues in the Department of Ocean Engineering for making my time at Texas A&M the best experience of my life.

Lastly, I would be remiss if I did not mention the abundant love and encouragement my family has given me throughout my endeavors. Their support in everything I do has been invaluable, and I am truly grateful.

CONTRIBUTORS AND FUNDING SOURCES

Contributors

This work was supervised by a thesis committee consisting of Dr. David Allen and Dr. Robert Randall of the Department of Ocean Engineering and Dr. Vinayak Krishnamurthy of the Department of Mechanical Engineering

All other work conducted for the research was completed by the student independently.

Funding Sources

Graduate support was provided by a donation to the Texas A&M Foundation

NOMENCLATURE

CIR	Center for Infrastructure Renewal
HDPE	High density polyethylene
FEMA	Federal Emergency Management Agency
RELLIS	Texas A&M University's Auxiliary Research Campus
USACE	United States Army Corps of Engineers

Any nomenclature regarding variables used in equations will be defined following the equation in the thesis.

TABLE OF CONTENTS

ABSTRACT.....	ii
DEDICATION	iii
ACKNOWLEDGEMENTS.....	iv
CONTRIBUTORS AND FUNDING SOURCES	v
NOMENCLATURE.....	vi
LIST OF FIGURES.....	x
LIST OF TABLES.....	xii
1. INTRODUCTION.....	1
1.1. Motivation.....	1
1.2. Background.....	3
2. POTENTIAL OCEAN ENGINEERING APPLICATIONS.....	5
2.1. Piers.....	6
2.2. Sea Walls	7
3. RESEARCH OBJECTIVES	9
3.1. Rationale for the Study	9
3.2. Rationale for Machinery Purchased.....	9
3.3. Experimental goal.....	10
4. EXPERIMENTAL METHODOLOGY	12
4.1. Forces induced on specimens	12
4.2. Calculation of Residual Stresses.....	14

5.	EXPERIMENTAL PROCEDURE	17
5.1	Equipment Used.....	17
5.1.1	Programs and equipment used in grip preparation	17
5.1.2	Programs and equipment used in material and specimen preparation	17
5.1.3	Equipment used in Machine preparation and testing.....	18
5.1.4	Programs and equipment used in inspection.....	18
5.1.5	Programs and equipment used for computational analysis.....	18
5.1.6	Lab safety equipment	18
5.2	Experimental Procedure.....	19
5.2.1	Grip preparation	19
5.2.2	Material and sample preparation.....	22
5.2.3	Machine Preparation	26
5.2.4	Inspection of Specimens	28
5.2.5	Post Mortem Inspection	28
6.	EXPERIMENTAL RESULTS	30
6.1.	Experimental Results from CIR Testing.....	30
6.1.1.	Specimen 1.....	31
6.1.2.	Specimen 2.....	34
6.1.3.	Specimen 3.....	36
6.2	Complications encountered	39
6.3	Conclusions from experimental tests.....	41
7.	COMPUTATIONAL ANALYSIS PROCEDURE.....	42
7.1	Grip induced stresses	42
7.2	Pore induced stresses.....	45
8.	FINITE ELEMENT AND STRESS ANALYSIS.....	51
8.1	Grip Analysis	51
8.2	Pore Analysis	54

9. RECOMMENDATIONS FOR FURTHER TESTING	57
10. CONCLUSION.....	59
REFERENCES	60

LIST OF FIGURES

Figure 1: Recycled HDPE glass fiber composite crosstie.....	4
Figure 2: Pier destruction after hurricane	5
Figure 3: Typical pier made of timber.....	6
Figure 4: Concrete seawall.....	7
Figure 5: Deflections on a crosstie as a result of a railcar	12
Figure 6: Warping in specimens cut from a crosstie	15
Figure 7: Physical representation of residual stresses in a specimen	15
Figure 8: Drawing of grips designed for experiment	19
Figure 9: Grips used with plate modification.....	20
Figure 10: metal plate designed and manufactured to modify wedge grips	21
Figure 11: Specimen area cut from crosstie	22
Figure 12: 3D Model of specimen with cross sectional dimensions.....	23
Figure 13: Distribution of widths throughout each specimen.....	24
Figure 14: Distribution of cross-sectional lengths throughout each specimen	25
Figure 15: Experimental fatigue testing of specimen	30
Figure 16: Force exerted on Specimen 1 over time.....	31
Figure 17: Specimen 1 post failure	32
Figure 18: Stress strain relationship in specimen 1	33
Figure 19: Force exerted on specimen 2 over time	34
Figure 20: Specimen 2 post failure	35
Figure 21: Stress strain relationship in Specimen 2.....	36

Figure 22: Force exerted on specimen 3 over time	37
Figure 23: Specimen 3 post failure	38
Figure 24: Crack propagation in Specimen 3	38
Figure 25: Stress strain relationship in Specimen 3.....	39
Figure 26: MTS fatigue testing machine in Ocean Engineering Materials and Structural Lab.....	40
Figure 27: Force applied to the specimen for computational analysis	44
Figure 28: Mesh of the specimen	45
Figure 29: Cross sectional view of HDPE glass fiber composite crosstie	46
Figure 30: Sample area taken for void statistics.....	47
Figure 31: Mesh of porous surface	49
Figure 32: Stresses induced by grips.....	52
Figure 33: Stresses induced by grips.....	52
Figure 34: Equivalent elastic strain in the specimen	53
Figure 35: Total deformation in the specimen	54
Figure 36: Stresses around the pores	55
Figure 38: Deformation on a porous surface.....	56

LIST OF TABLES

Table 1: Sample Statistics	25
Table 2: Material Property Inputs for HDPE Glass Fiber Composite	42
Table 3: Material Properties of Steel	43
Table 4: Pore Statistics	48

1. INTRODUCTION

This thesis will focus on how HDPE glass fiber composite specimens cut from beams are affected by cyclic loadings by experimentally modeling the fatigue behavior. The beams tested have a proposed use for railway crossties, construction mats, piers, docks, seawalls, and several other applications in coastal environments. Samples of the composite material tested were cut from full scale beams and subject to constant amplitude uniaxial fatigue testing.

Throughout the duration of the experiments, a literature review was conducted to gather information on materials used in the previously mentioned applications. The literature review is represented and referenced throughout the entire thesis. Data collected from the review was used to create a comparison of the HDPE glass fiber composite with methods and materials currently in place. In order to carry out further experiments, the necessary equipment was purchased, installed and calibrated.

1.1. Motivation

Currently, many industries are predominantly using wooden beams for structural support, such as crossties, piers and construction mats. This is due to the availability, inexpensive cost, easy installation of wooden beams as crossties, and longevity of the practice. However, many issues can arise when using timber. These issues increase significantly in coastal areas.

For example, consider wooden piles used for piers. Untreated wood has “insufficient decay and infestation resistance for these exposures” according to the Coastal Construction Manual published by FEMA. Because of this, the wood must be pressure treated with creosote, a preservative used to prevent rotting of the wood. This is done in order to provide the minimum structural integrity needed to support a structure and bear any loads. However, even when treated with creosote, these wooden beams are subject to splitting, plate cutting, spike pull, insect infestation, and rotting. IN addition, creosote is an environmental hazard.

Splitting and cracking in timber is a potentially detrimental, yet very common issue encountered in the field. This problem is greatly exacerbated in high pressure, high force environments, such as on railroads. The average loaded railway car exerts a pressure of roughly 1500 pounds per square inch on a crosstie. According to an article published by BNSF Railway Company entitled “Class I Railroads Continue the Longer Train Trend,” the average number of cars on a train in 2018 was 173 cars. In addition, the minimum number of axles on a train car is four, but the number of axles can be increased to as many as twelve. With this, it can be determined that the average train exerts roughly 1,400 fatigue cycles on a crosstie as it runs over the track. In addition, the number of cars and boxes on a train is steadily increasing, meaning railway ties are being introduced to more and more forces, resulting in a shorter life span and need to be replaced more frequently.

Due to the issues encountered, this practice of using wooden beams is becoming outdated as better solutions hit the market. Among these better solutions is a recycled polyethylene glass fiber composite material that offers more strength and durability, thus in

return, a longer lifespan. Unlike timber, the composite material cannot absorb water, and therefore is immune to deformations experienced due to the intake of water in coastal environments. The recycled HDPE glass fiber composite material is estimated to have greater strength and durability than wood, while retaining the light weight and ductile nature of timber.

1.2. Background

The composite material being tested is made from recycled HDPE and glass fiber. The recycled HDPE is melted down to a viscous state, then the glass fibers are added to the mixture. The mixture is then injected into a mold with a blowing agent, where it forms a thick, solid outer layer and porous interior as it cools. Due to the blowing agent the number and size of pores within the beam varies spatially, and the glass fibers are distributed in a random pattern and orientation. Following the fabrication of the crosstie, it is subjected to a visual inspection as well as an x-ray to identify any defects in the material that could potentially render it unsafe for use in the field.

Recently there has been an increasing interest by companies to look to “greener” alternatives in the way they operate. The manufacturer of this recycled HDPE glass fiber composite is no exception to this initiative, as newly developed material is made from 100% recycled HDPE. In addition, if a composite crosstie is produced but does not pass the safety inspection, the material from the crosstie, though already molded and cast, can also be cut up, recycled, and used to create a new composite beam. A cross sectional view of a crosstie

is seen in Figure 1, which depicts the variation and random pattern of the pore distribution in the center of the cross tie, as well as the solid exterior.



Figure 1: Recycled HDPE glass fiber composite crossie

2. POTENTIAL OCEAN ENGINEERING APPLICATIONS

In the midst of several 100 and even 1000-year storms that have occurred recently in our oceans and on our coasts, there is a dire need for a stronger, more durable, readily available material used for structures in coastal regions, as current structural components used are succumbing to these natural disasters, as indicated in Figure 2.



Figure 2: Pier destruction after hurricane

Because each region is so morphologically diverse, the material used in construction of structures varies from place to place, as well as from project to project. Smaller projects such as personal docks, rely heavily on timber due to its availability, inexpensive cost, and ease to work

with. The composite polymer material presented in this research is offers a low cost of manufacturing, is considerably more durable, and it can be adapted its surroundings while greatly reducing installation costs.

2.1. Piers

Due to the superior material and structural properties of the HDPE glass fiber composite, the material has potential to be used in a wide array of possibilities in ocean engineering. More specifically, in coastal structures, this material is a promising alternative to timber for applications on piers, docks and marinas, as seen in Figure 3.



Figure 3: Typical pier made of timber

Before use in coastal environments, timber is pressure treated using creosote, a potentially harmful chemical, to strengthen and prohibit waterlogging in the structural elements. Due to the plastic nature of the HDPE glass fiber composite, it is impervious to water, therefore it does not experience the same detrimental degradation in coastal environments, unlike its timber counterpart.

2.2. Sea Walls

In addition to timber, reinforced concrete is also widely used in coastal structures such as piers and seawalls, depicted in Figure 4. Though commonly used, reinforced concrete has significantly larger installation costs and higher costs of failure.



Figure 4: Concrete seawall

The composite beam structures offer a more cost-effective solution to this. For example, when a concrete structure begins to crack, the entire structure is compromised. However, if a crack were to propagate from one composite beam, the beam could be easily replaced, rather than replacing the whole structure. In doing this, not only is the monetary cost significantly less, but the time cost to take our and reinstall the structural component is reduced greatly as well.

In addition, when the material needs to be replaced, unlike timber and concrete, the beams can be easily be recycled by melting down the existing beam and repeating the manufacturing steps to creating the composite beam as previously touched on. Then, the material is formed into new beams, and put back into the field, offering a more cost effective and an environmentally friendly alternative to the current methods of coastal construction.

3. RESEARCH OBJECTIVES

3.1. Rationale for the Study

An HDPE glass fiber composite material intended for use as railway crossties and construction mats is studied herein. Limited data exists for this material, given its unique design and recently emerging presence in the field. The facilities at Texas A&M offer a wide range of testing capabilities, including uniaxial fatigue testing. For this reason, the study was to be conducted using testing equipment housed within the Center for Infrastructure Renewal on Texas A&M's RELLIS campus and the Ocean Engineering Materials Lab on the main campus at Texas A&M.

3.2. Rationale for Machinery Purchased

The experiments were conducted at Texas A&M RELLIS campus' Center for Infrastructure Renewal (CIR). However, due to an influx of projects taking place at the CIR, there was a shortage of machinery and personnel available. To compensate for the lack of machine availability, the department of Ocean Engineering approved the purchase of a new MTS 812.21 fatigue rated, uniaxial testing frame capable of producing 3.3 kips of force. Many requirements were taken into consideration when purchasing the appropriate machinery. The requirements taken into consideration included:

1. Uniaxial loading and displacement capabilities

- a. Ability to test in tension.
2. Capability of exerting a minimum of 2000 pounds of force
3. Able to perform cyclic fatigue experiments
4. Minimum gauge length of 14 inches
5. Closed loop power source (hydraulic or electric)

Other non-technical requirements, such as machine dimensions, price, and company reliability were also taken into consideration.

3.3. Experimental goal

The goal of this research is to 1) gain a better understanding of the behavior of a polymer composite comprised of recycled HDPE and glass fibers, and 2) obtain values for the material properties through experimental uniaxial fatigue testing. Following the experiments, the data will be compiled, analyzed and interpreted, resulting in pertinent information regarding how the material is expected to behave in the field. After the analysis of experimental data, recommendations will be made regarding recommendations for future testing and the material itself. In addition to providing recommendation for further testing, the goal of the experiment is to ascertain if there are potential improvements in the fatigue performance of the composite crossties.

Using the information gathered from the experiments, a further comparison will be made to other materials currently used in potential applications for the polymer composite.

More specifically, comparing the material to the materials commonly used in the railway industry, where composite materials have already been introduced.

Another purpose of this experiment is to determine potential applications for the polymer composite to ocean applications, such as coastal structures. For example, it is anticipated that the water resistant, impervious HPDE glass fiber composite material has great potential for deployment in coastal environments.

4. EXPERIMENTAL METHODOLOGY

4.1. Forces induced on specimens

The goal of this portion of the research is to simulate the forces induced on a crosstie at the moment a train car passes over it. In order to achieve this, the pressure induced by a loaded rail car on a crosstie needs to be calculated. There are many factors taken into consideration when determining the stresses experienced in a crosstie. For example, though the weight of a train car may be known, the rails and crossties are not the only mediums impacted. The force is dispersed throughout the rails and crossties and into whatever medium lies underneath it, whether it be ballast, soil and/or sand. Figure 5, illustrates the deflections experienced by a crosstie due to loading induced by a railcar.

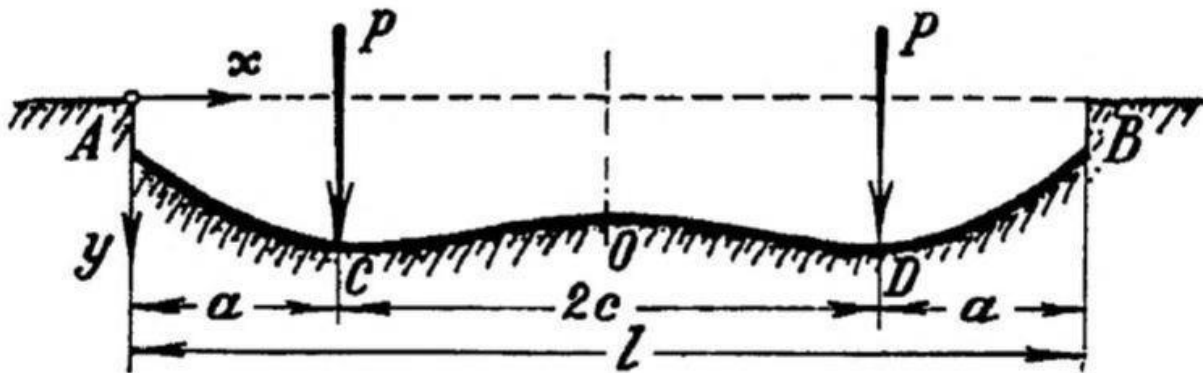


Figure 5: Deflections on a crosstie as a result of a railcar

The bending moment equation for the crosstie above can be calculated mathematically using equations (1) and (2).

$$M_{A-C} = \frac{P}{2\lambda} \frac{1}{\sinh \lambda l + \sin \lambda l} \{2 \sinh \lambda x \sin \lambda x [\cosh \lambda a \cos \lambda(l-a) + \cosh \lambda(l-a) \cos \lambda a] +$$

$$(\cosh \lambda x \sin \lambda x - \sinh \lambda x \cos \lambda x)[\cosh \lambda a \sin \lambda(l-a) - \sinh \lambda a \cos \lambda(l-a) +$$

$$\cosh \lambda(l-a) \sin \lambda a - \sinh \lambda(l-a) \cos \lambda a]\}$$
 (1)

$$M_{C-D} = [M_{A-C}]_{x>a} - \frac{P}{2\lambda} [\cosh \lambda(x-a) \sin \lambda(x-a) + \sinh \lambda(x-a) \cos \lambda(x-a)]$$
 (2)

where M is the bending moment, P is the point load, and a , x and l are length parameters defined in Figure 5.

To obtain values for the moments, the parameter λ is defined using as follows

$$\lambda = \left(\frac{k}{4EI} \right)^{\frac{1}{4}}$$
 (3)

where E represents the modulus of elasticity for the HDPE glass fiber composite beam, I is the moment of inertia, and k represents the elastic modulus of the foundation material the crosstie rests on. In this experiment, the maximum stress is needed to determine the maximum loading on the specimens. As a result, a conservative value of k is used, and is assumed to be 100 MPa, or roughly 14,500 psi.

For this research, it is assumed that the modulus of elasticity of the material is equal to 250,000 psi. The moment of inertia is calculated using the cross-sectional area of the beam and the equation(4). For this experiment, we assume the standard dimensions of a crosstie to be 7 in. X 9 in. X 108 in.

$$I = \frac{bh^3}{12} = \frac{9 [in] * 7^3 [in]}{12} = 257.25 [in^4]$$
 (4)

The typical load imparted onto the crosstie by a boxcar wheel defined as point load, P , is roughly 160 kN, which is equivalent to 35969 lbs. The average value for a is 25.75 inches.

Lastly, the stresses induced on a crosstie when a rail car passes over can be calculated using

$$\sigma_n = \frac{My}{I} \quad (5)$$

where σ_n represents the stress in the crosstie, M represents the internal moment, y represents the distance from the centroid of the cross section and I represents the second area moment of inertia of the cross section. Applying those values results in a maximum normal stress of 1500 psi. This value was used to determine the loading amplitude to the test specimens.

4.2 Calculation of Residual Stresses

When the specimens were cut from the crossties, there was a slight warping in the specimens. Figure 6 displays an example of the warping that occurred when cut from the crosstie. The warping of the material indicated that there are residual stresses are caused by compression on the interior cut and tension on the exterior surface of the specimen. Therefore, when the specimen is loaded in tension in the testing frame, as shown in Figure 7, those stresses have an effect on the fatigue behavior.

Full Scale Cross Tie
Specimen

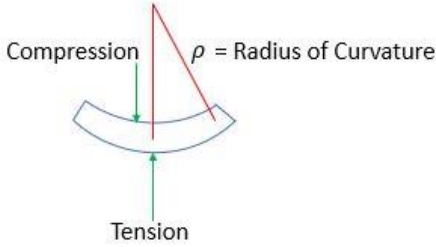


Figure 6: Warping in specimens cut from a crosstie



Figure 7: Physical representation of residual stresses in a specimen

The residual stresses can be calculated as a function of the radius of curvature in the equations below, where ρ represents the radius of curvature, M represents the bending moment, E represents the modulus of elasticity, and I represents the moment of inertia.

$$\frac{1}{\rho} = \frac{M}{EI} \tag{6}$$

For the specimens used in this experiment, the modulus of elasticity and bending moment of inertia are assumed to remain constant with $E = 250,000$ psi and the moment of inertia as calculated below.

(7)

$$I = \frac{bh^3}{12} = \frac{1.5(0.75)^3}{12} = 0.0527 \text{ in}^4$$

To find the residual stress as a function of the radius of curvature, the following equation can be used where $\Delta\sigma$ represents the residual stresses and y represents the distance to the centroid of the cross section.

$$\Delta\sigma = \frac{My}{I} \quad (8)$$

Applying the equation for M results in the following equation

$$\Delta\sigma = \frac{EI}{\rho} \frac{y}{I} \quad (9)$$

The moment of inertia cancels out, resulting in the equation

$$\Delta\sigma = \frac{Ey}{\rho} \quad (10)$$

Applying the equations for the constants for this experiment, the residual stress due to warping as a function of the radius of curvature at the outer surface is found to be

$$\Delta\sigma = \frac{250,000 (0.375)}{\rho} = \frac{93750}{\rho} \text{ psi} \quad (11)$$

Using the calculated residual stresses, the total stress experienced in the specimen during experimentation can be calculated by superposing the stress induced by the machine and the residual stresses as inferred in equation (12) where σ_M is the stress resulting from forces applied by the experiment as a function of y , which should be 1500 psi and σ_T is the total stress.

$$\sigma_T = \sigma_M + \Delta\sigma \quad (12)$$

5. EXPERIMENTAL PROCEDURE

5.1 Equipment Used

A variety of equipment was used during different phases of the research. The equipment and programs used have been listed below in the order they were utilized.

5.1.1 Programs and equipment used in grip preparation

- SolidWorks Academic License
- Two 2.5-in. diameter X 1.6 in. tall cylinders of 4140 heat treated steel
- Computer Numerically Controlled (CNC) steel milling machine
- 2-inch diameter cylindrical grip adapters
- 6 in. X 6 in. X ¼ in. sheet of 4140 heat treated steel
- Water jet
- ¾ in. Allen wrench

5.1.2 Programs and equipment used in material and specimen preparation

- 7 in. X 9 in. X 96 in. recycled HDPE glass fiber composite crosstie
- Table saw
- Calipers
- Microsoft Excel
- Sanding belt
- Wood planar

5.1.3 Equipment used in Machine preparation and testing

- MTS tension fatigue rated testing frame with 22-kip capacity actuators of 6-in. stroke
- Hydraulic pump unit
- MTS FlexTest digital controller
- MTS TestSuite software
- 1.5 in. X 0.75 in. X 12 in. recycled HDPE glass fiber composite sample

5.1.4 Programs and equipment used in inspection

- Magnifying glass
- CT scanner
- ImageJ CT compatible software
- Calipers

5.1.5 Programs and equipment used for computational analysis

- ANSYS Academic License
- Python
- Autodesk Fusion360
- Recycled HDPE glass fiber composite cross section of railway crosstie

5.1.6 Lab safety equipment

- Protective eyewear
- Steel toed shoes
- Gloves (only necessary when working with sanding belt)

5.2 Experimental Procedure

5.2.1 Grip preparation

The machinery and tests frames made available to us for this research came equipped with grips. However, none of the available grips could accommodate the minimum specimen cross sectional area of 1 in^2 required to conduct the experiments. Due to this complication, new grips needed to be manufactured and existing grips needed to be modified to accommodate the test specimens. After working with personnel at the RELLIS Campus to determine a specimen size that could work with a set of grips designed by the research team to compliment an adapter for the test frame, the grip design, shown in Figure 8 was determined to be the best fit.

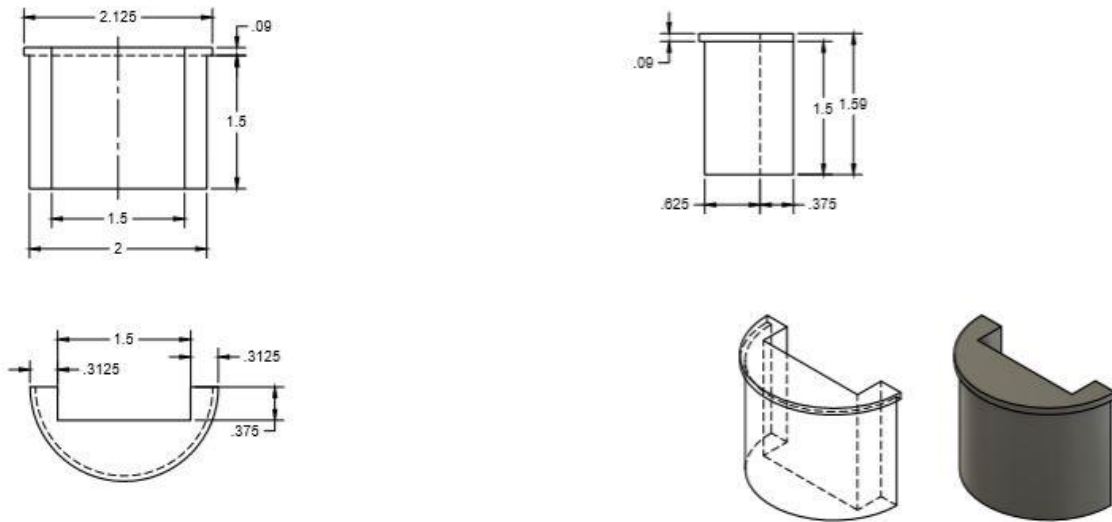


Figure 8: Drawing of grips designed for experiment

The grip design was taken to Brazos Valley Drivelines to manufacture 2 sets of grips, four pieces total from 4140 heat treated steel. The grips were then brought to the RELIS campus to begin testing. These grips work by being inserted into the test frame's grip adapters. Once in the adapters, the specimen is then inserted into the top grips, the hydraulics of the frame are turned on, and the two grips compress the sample to hold it tightly in place. The machine's crosshead is then moved up and the bottom end of the specimen is placed in the grips. Similar to the top, the grips are then compressed around the sample to gain a tight hold to avoid any slipping throughout the duration of the experiments.

Another set of grip was used for the larger MTS machine at RELIS, however, modifications to existing grips were required. The grips available worked by using the hydraulic power and cross-head movement to push two steel wedges up to tightly grip onto the sample, similar to the ones shown in the drawing in Figure 9.

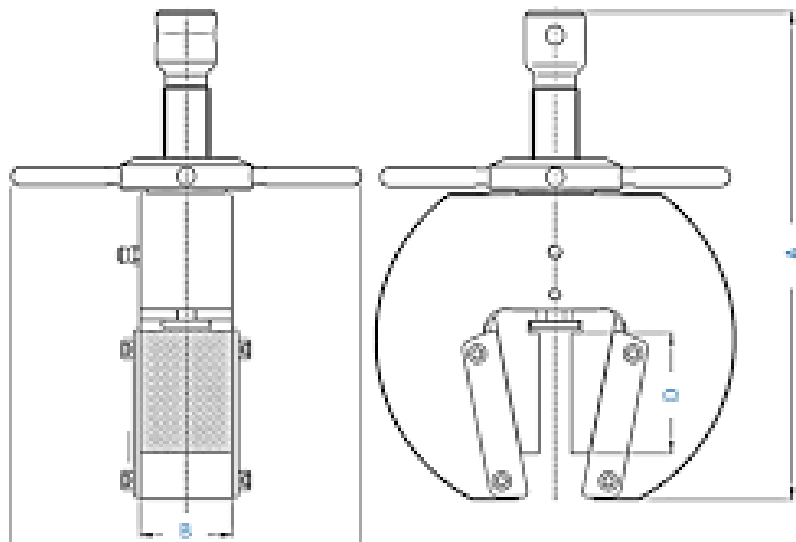


Figure 9: Grips used with plate modification

In order to properly and tightly grip the specimens for the experiments, two metal plates were required to be added between the grips and wedges in order to decrease the spacing between the two wedges that hold the specimen. This plate was designed by taking measurements of the available opening in the grips where the plate would be inserted, and measuring the necessary minimum thickness needed to set the wedges at an appropriate spacing. The drawing depicted in Figure 10 was constructed and sent to the water jet machine where the metal plate insert was cut. Following the cut, the grips were disassembled and reassembled with the plate.

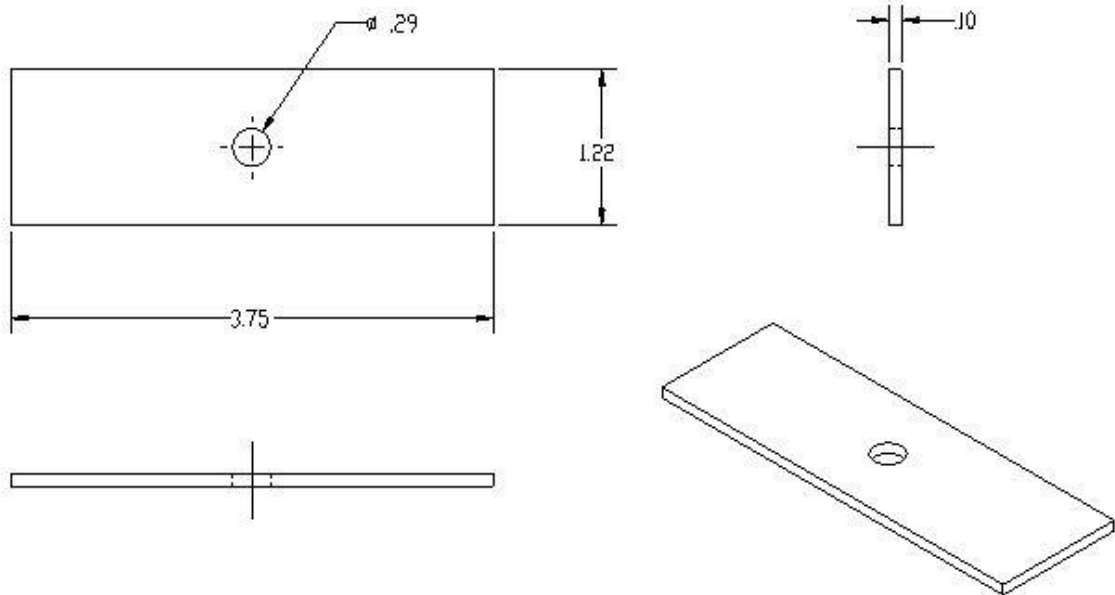


Figure 10: metal plate designed and manufactured to modify wedge grips

5.2.2 Material and sample preparation

As Previously stated, the recycled HDPE glass fiber composite is created by melting the recycled HDPE to a liquid state, adding glass fibers, mixing the melted material, and injecting the mixture into a mold. Samples for this experiment were cut from the underside, outermost, center of a crosstie, as that is where the largest stress occurs is when the crossties are implemented in the field. This is illustrated in Figure 11 with the red section indicating where the sample is extracted.

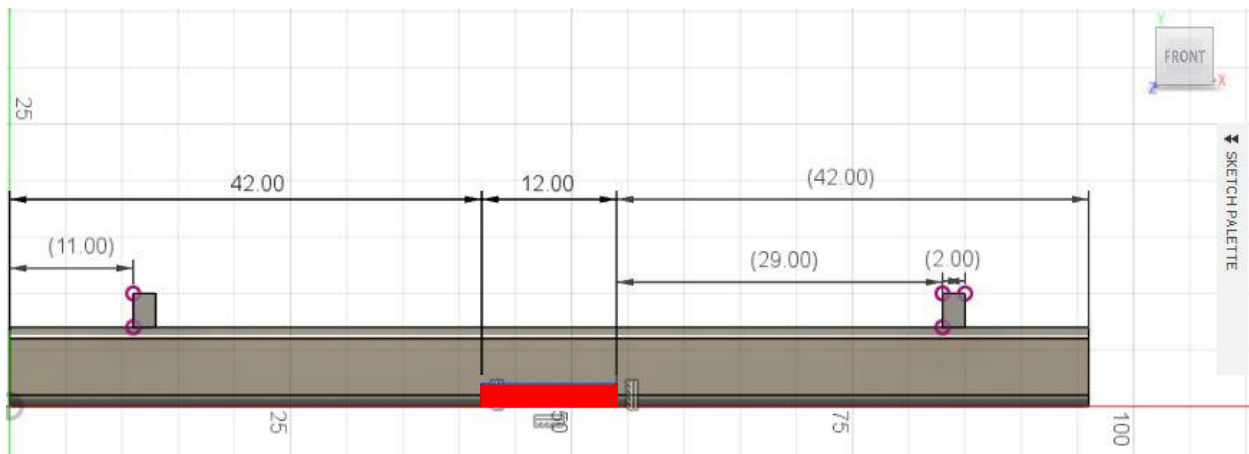


Figure 11: Specimen area cut from crosstie

Several factors contributed to the specimen size decided upon for these experiments. These factors include gauge length allowed by the machine, the grips available, and the necessary cross-sectional area to maintain constant force exerted by the machinery used. Given these factors, it was determined that the specimen required a minimum cross-sectional area of 1 in^2 . When taking into account the grips needed to use the machine were required to have a diameter of 2 in, it was determined that the ideal dimension of the specimens would be 0.75 in. X 1.5 in. X 12 in., as seen in the schematic in Figure 12.

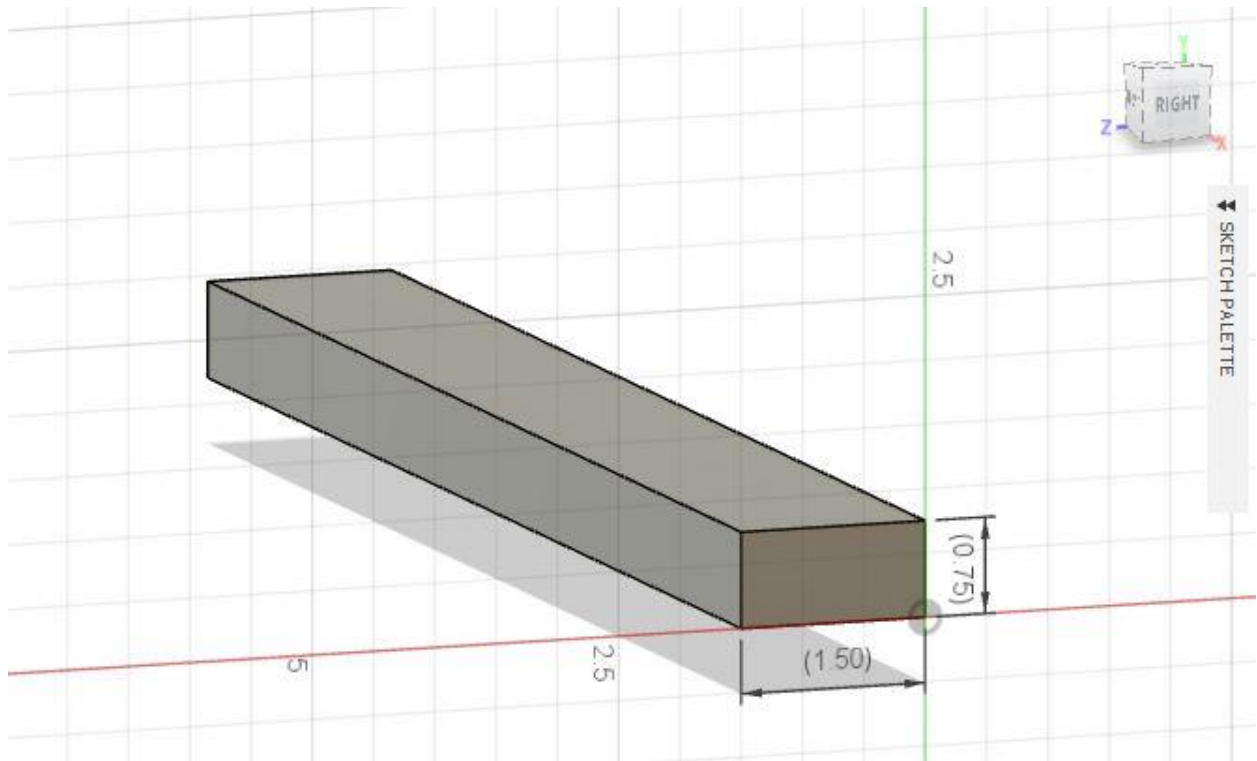


Figure 12: 3D Model of specimen with cross sectional dimensions

Each specimen was numbered and the cross-sectional dimensions were measured at 0, 3, 6, 9 and 12 in. along the length of the specimen. The specimens varied greatly in size as well as throughout each individual specimen. Figure 13 represents how the specimens varied in cross sectional width, with the green line representing the dimensions needed to accurately complete testing. The width was fairly consistent within each specimen, but varied greatly across the specimen population.

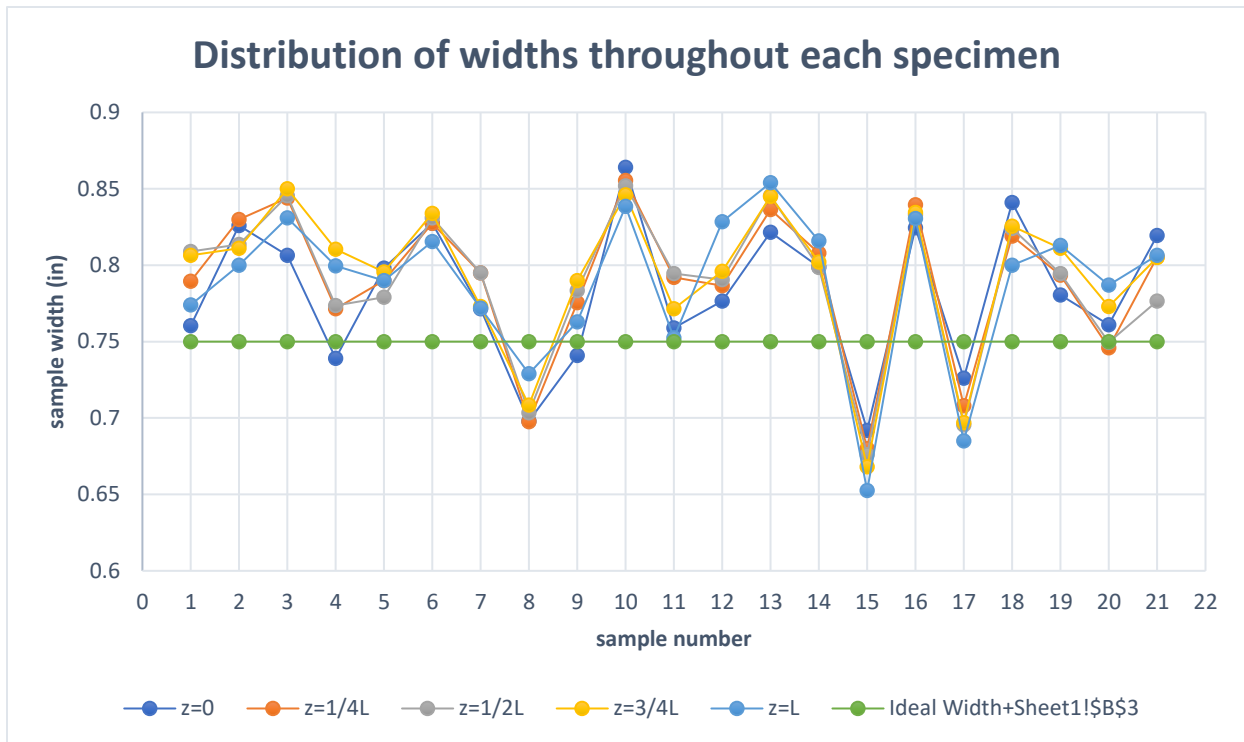


Figure 13: Distribution of widths throughout each specimen

Similarly, the sample length also varied across the sample population. However, unlike the sample width, there was very little consistency in the length of each individual sample. As seen in Figure 14, all sample lengths were greater than the desired length, resulting in the need for the specimens to be cut down further to accommodate the experiments. Table 1 shows the length statistics of the samples.

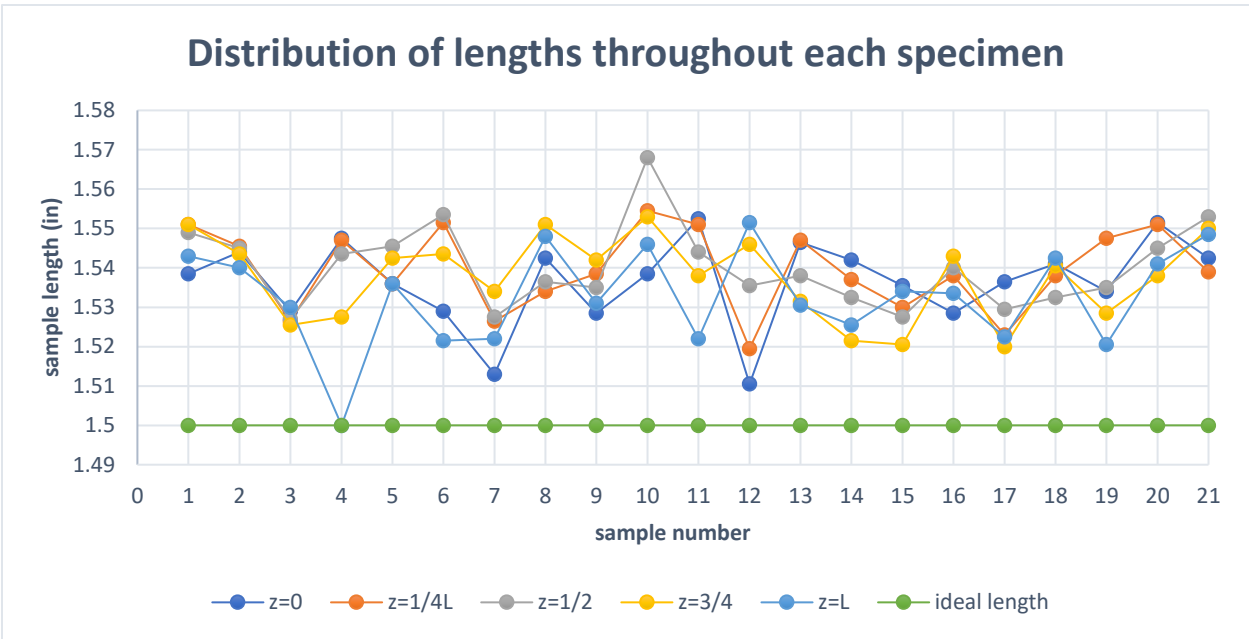


Figure 14: Distribution of cross-sectional lengths throughout each specimen

Table 1: Sample Statistics

.	Cross Sectional Length	Cross Sectional Width	Cross Sectional Area
Min	1.5000	0.6525	1.0326
Max	1.5680	0.8500	1.3359
Mean	1.5375	0.7825	1.2149
Median	1.5378	0.7805	1.2195
Variance	0.0001	0.0022	0.0061
Stan. Dev.	0.0109	0.0467	0.0781

This variation in cross-sectional length and width resulted in a new preparation plan for the materials and it was necessary to acquire additional equipment. Initially, samples that did not fit in the grips were sanded down using a belt sander. However, due to a lack of ability to apply constant pressure throughout the entire specimen while sanding, the specimens still varied in size. Upon further research, it was determined the best method of

obtaining constant size in all specimens would be through the use of a planar. A planar was purchased specifically for the use of this experiment, as it offered size settings that were capable of being locked to ensure consistent, uniform cuts for all specimens.

After planing all specimens down to a uniform thickness and width, each was subjected to a visual inspection, where external pores, deformities and material abnormalities were noted. The specimens were also measured again to the 0.0001 in accuracy at the various points aforementioned to ensure the correct stresses would be applied during testing.

Lastly, a visual inspection of the material was conducted. All defects, abnormalities and pores were noted, along with their location, as these represent potential fracture sites.

5.2.3 Machine Preparation

Once the samples were mounted into the machine for testing, a testing protocol was created for each sample. After each specimen was planed down to the appropriate size, the specimens were remeasured prior to being inserted into the machine. Using the measurements at the cross section prior to being inserted into the machine, the cross-sectional area was calculated, thereby dictating the exact maximum load amplitude the sample should encounter during the experiment. The following simple equations were used to determine the machine inputs, where L represents cross-sectional length in in., W represents cross sectional width in in., A represents the cross-sectional area in in^2 , σ represents the stress in psi, and F represents the force exerted in lbf.

Equation (13) Cross sectional area taken at the center of the specimen

$$A = L \times W \quad (13)$$

Equation (14) Force required to apply desired stress of 2000 psi

$$F = \sigma A \quad (14)$$

A program was created within the machines control panel for the purpose of testing the specimens. After calculating the force required to induce stresses of 2000 psi, the force was then input into the program. Following a force input, the program was modified to ensure a zero-based loading, meaning the specimen would only be tested in tension within a range of 0 to 2000 psi, thereby ensuring that the specimen does not experience any compression. Also included in the program was a command to run the experiment as a fatigue test, in the process creating a sinusoidal load history. Next the desired number of cycles was specified. For this experiment, the machine was programmed to run 100,000 cycles and cease testing once that number was reached. A condition was added to stop the machine from running if there was a sudden increase in displacement, indicating that the sample either slipped from the grips or fractured. Lastly, the cycle frequency was input. For our case, the frequency the experiments were to be conducted at was 3 hz. Once both the specimen was in place and the program was appropriately modified for the specimen, each experiment was initiated.

5.2.4 Inspection of Specimens

Throughout the duration of the experiments, the specimens were to be taken out of the testing frame every 100,000 cycles for inspection. This inspection was to include a visual inspection of the exterior of the specimen. Similar to the visual inspection prior to testing, the inspector was to look for defects and any abnormalities. However, the visual inspection in between testing also required noting any changes in the cross-sectional area, increase in pore sizes (if pores were present), and any indication of external crack propagation.

After the external visual inspection was completed, the samples were taken to the Richardson Petroleum Engineering lab, where the specimen underwent a CT scan. The CT scan was then compiled in a program called "image J," which allows the user to visualize the specimen in three dimensions. Using this program, the user can see the interior portion of the sample as well. Using the scans, an internal visual inspection of the material was also conducted. In this internal inspection, the user can search for any indication of internal crack propagation, or any other source of internal deformations that could result in the fracture and/or failure of the specimen.

5.2.5 Post Mortem Inspection

After the specimen fractured, a post mortem inspection was conducted to better understand the nature, of the specimen failure. Some elements noted in this inspection are the suspected origin and cause of failure in the specimen. For example, the post mortem inspection was compared to the notes taken from the visual inspection that occurred before the sample underwent testing. This would indicate if the failure was a result of an existing

defect, or if cracks had propagated from an existing pore in the material caused by the blowing agent.

In addition, the post mortem tests revealed much about the materials properties, depending on the mode of failure. For example, the inspection could reveal if the material was more ductile or brittle depending on the deformations experienced leading up to the specimen failure. If there is a significant change, or thinning in the specimen's cross-sectional area near the fracture, it would indicate a ductile failure, similar to that of many plastics and polymers. However, a clean break with little to no deformation would indicate a brittle fracture.

Following the inspection of the failure point, the specimen was inspected for other possible sources of failure, such as cracks that formed in other areas prior to the specimen failure.

6. EXPERIMENTAL RESULTS

6.1. Experimental Results from CIR Testing

This experiment was conducted at the Structural and Materials Testing lab on Texas A&M University's RELLIS campus. The experiments were performed using two 22-kip MTS tension fatigue rated testing frames, pictured in Figure 15. In these experiments, samples taken from the HPDE glass fiber crosssties were subjected to sinusoidal cyclic, load-controlled fatigue tests to determine the fatigue life and material properties of the composite material. A better understanding of the material's behavior when subjected to cyclical fatigue was gained as well.



Figure 15: Experimental fatigue testing of specimen

As stated in our procedure, the samples were subjected to sinusoidal loading that result in the cross-sectional area experiencing stress of roughly 2000 psi, the maximum stress value a fully loaded railway car would induce on that location in the crosstie. Also, as stated in the procedure, the samples were to run to one million cycles, with an inspection every 100,000 cycles. However, shortly after testing began, it became evident that the initial procedure would not be a viable option, as the specimens that were tested all failed within 5,000 cycles. However, the samples tested did provide great insight into the material behavior and changes that could be made to increase the strength and fatigue life.

6.1.1. Specimen 1

In the first specimen tested, the cross-sectional area was calculated to be 1.12 square inches, resulting in a maximum force loading of 2220 pounds needed to achieve the desired stress of 2000 psi. As shown in the sinusoidal pattern in Figure 16, the machine was able to maintain nearly a zero, based loading, as well as keeping a consistent peak loading.

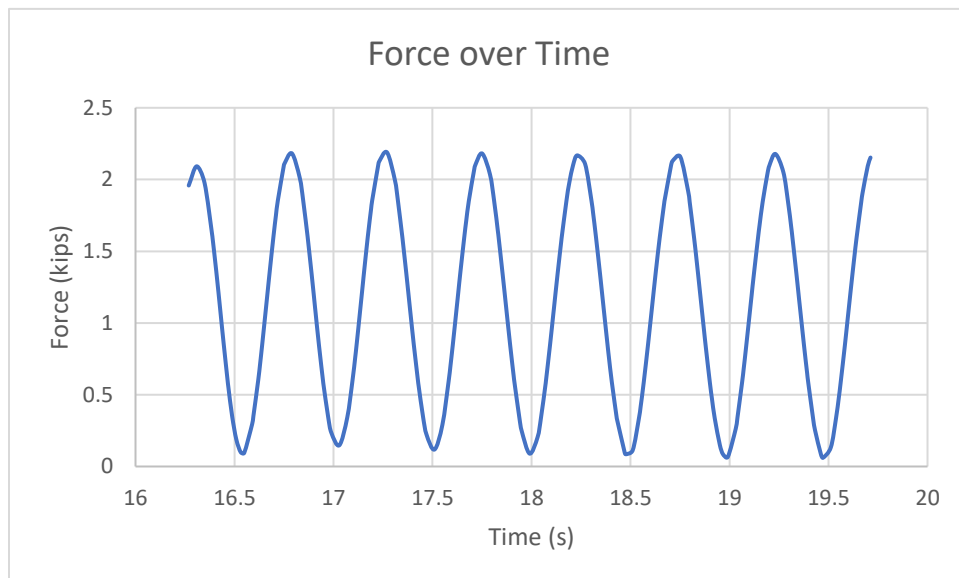


Figure 16: Force exerted on Specimen 1 over time

Upon visual inspection before subjecting the specimen to the fatigue tests, it was noted that there were numerous pores, both on the interior of the sample, as well as the exterior on one side. The defects in the sample can be attributed to the blowing process into the mold, which creates a porous center in the crossties, but leaves a hard-outer shell. As seen in the image of specimen 1 in figure 17, the crosstie exhibited larger pores and deformities of abnormal shapes just under the surface of the interior edge.

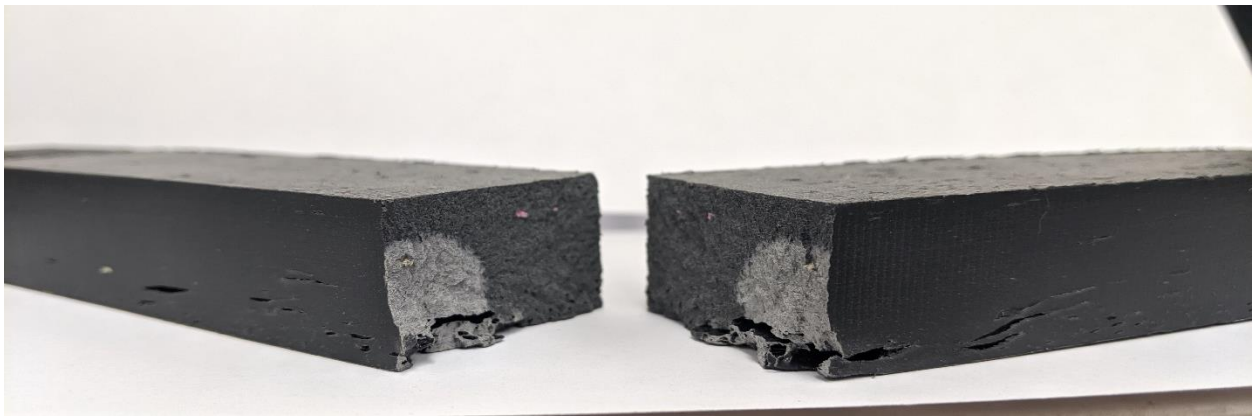


Figure 17: Specimen 1 post failure

Ultimately, the defect is what led to an early fracture of the material 3517 cycles into the experiment. What is also made evident in Figure 19 is the difference in coloration of the cross-sectional area, indicating where the initial fracture took place. The lighter color and slight elongation in the material surrounding the point of failure suggests a ductile fracture in that area that had been slowly separated over time, whereas the darker area suggests a brittle fracture throughout the remainder of the specimen's cross section.

Furthermore, given the data extracted from the program used to conduct the experiments, the Young's modulus for the material was obtained. This was obtained using the

stress experienced in the cross-sectional area by using the axial forces generated by the MTS machine and the cross-sectional area. Using equation (14), values for stress experienced at each cycle was recorded. Secondly, the strain was obtained by using equation (13), which utilizes the overall length of the specimen, 10 in., and the axial displacement measured by the MTS machine's linear variable differential transformer (LVDT). Using these values, a uniaxial stress-strain curve was obtained. A line of best fit was generated to determine the Young's modulus of the material, as seen in figure 18. The Young's modulus recorded for the material in this specimen was 240,100 psi.

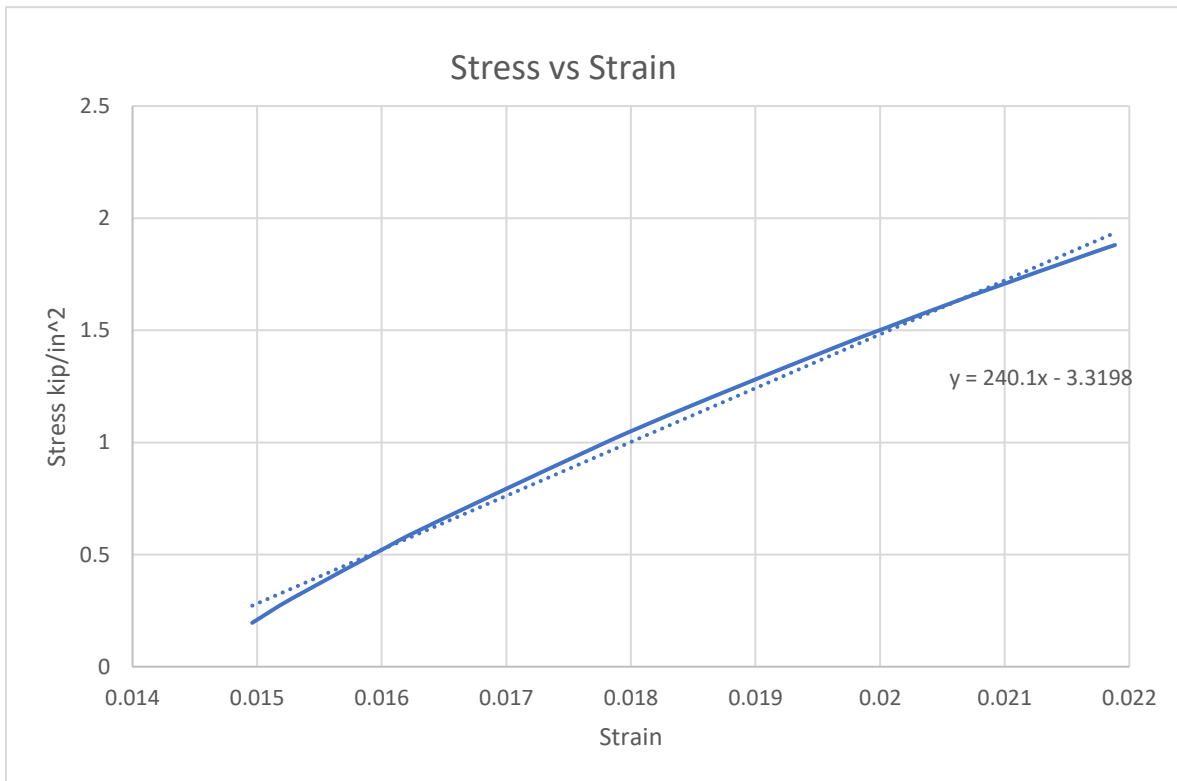


Figure 18: Stress strain relationship in specimen 1

6.1.2. Specimen 2

In the second specimen tested, the cross-sectional area was calculated to be 1.11 square inches, resulting in a maximum force loading of 2342 pounds needed to achieve the desired stress of 2000 psi. Similar to specimen 1, a sinusoidal, cyclical loading pattern depicted in Figure 19. However, it differs from specimen 1 in the sense that there is some error and variation in the peak and valley values of the loading. Despite the slight error, the figure indicates that specimen 2 never went into compression loading, and the peaks and valleys seemingly evened out to a more consistent pattern as the experiment proceeded.

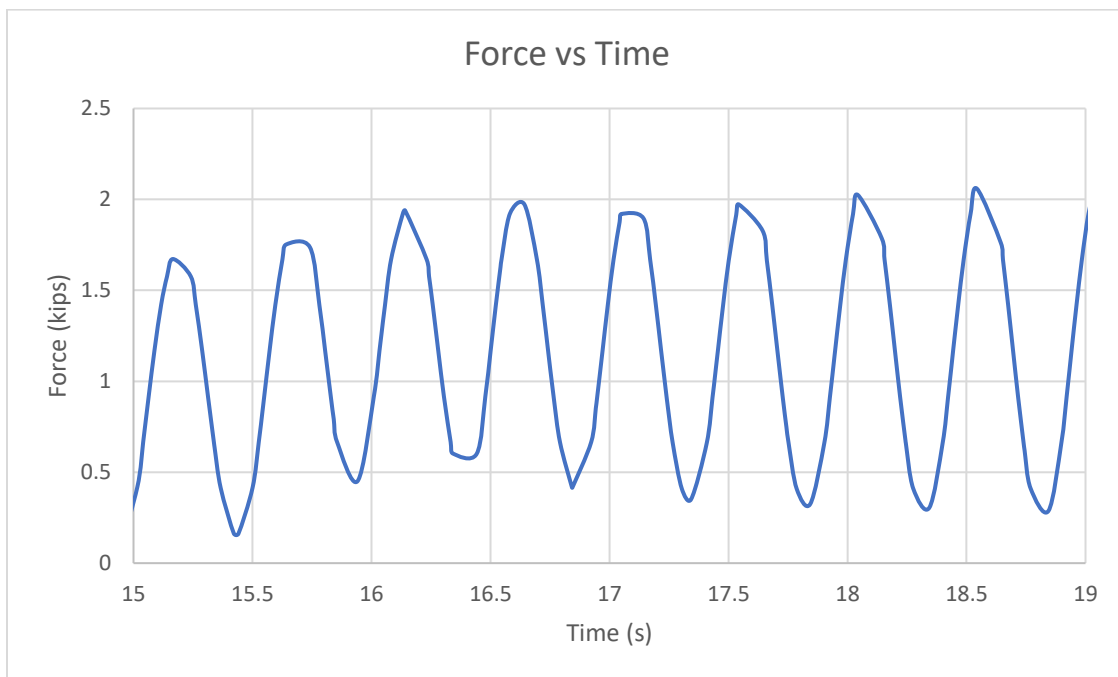


Figure 19: Force exerted on specimen 2 over time

Before running the experiment, specimen 2 was subjected to a visual inspection. In the visual inspection, abnormally large and sharp pores were noted on the surface of the specimen. Similarly, to the case with specimen 1, the defect could be attributed to the injection process.

This pore is where the crack that resulted in failure originated. However, upon fracturing, it was discovered that though small on the outside, the void penetrated much deeper into the material in an abnormal fashion, unlike the spherical pores seen throughout most of the specimens. This can be seen in Figure 20.



Figure 20: Specimen 2 post failure

As seen in Figure 20, there were many more abnormally shaped voids on the interior of the material. The lighter portion of the interior, which we earlier defined as a ductile fracture, takes an interesting pattern in specimen 2, as it does not surround only the origin of the failure, but also the internal voids. This indicates that a surface crack, combined with an internal crack or cracks, may have caused the failure of this sample. It is also worth noting that the figure above clearly shows another crack propagating on the surface of specimen 2. The crack is visible on the center of the side of the left half of specimen 2. Despite the larger number of cracks propagating through the specimen, the fatigue life of specimen 2 exceeded the fatigue life of specimen 1, with a count of 3947 cycles before failure and a slightly higher modulus of elasticity of roughly 248,500 psi as shown in Figure 21.

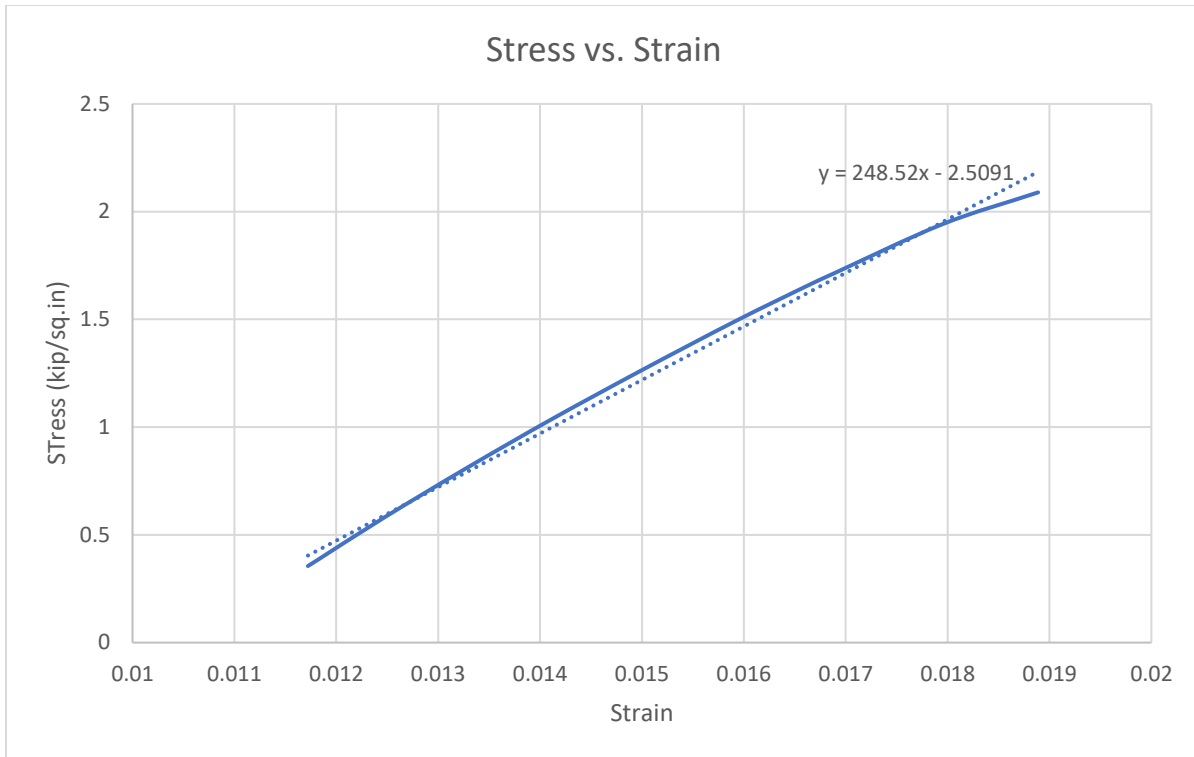


Figure 21: Stress strain relationship in Specimen 2

6.1.3. Specimen 3

Lastly, in specimen 3, a cross sectional area of 0.99 inches was measured, resulting in a maximum loading force of 1972 pounds needed to achieve an internal stress of 2000 psi. The sinusoidal relationship between the force and running time of the experiment shown in Figure 22 shows the cyclical nature of the fatigue tests, similar to the previously tested specimens. The data was extracted between 15 and 20 seconds into the experiment, which accounts for the gradual increase and stabilization of the peak values exerted on the specimen.

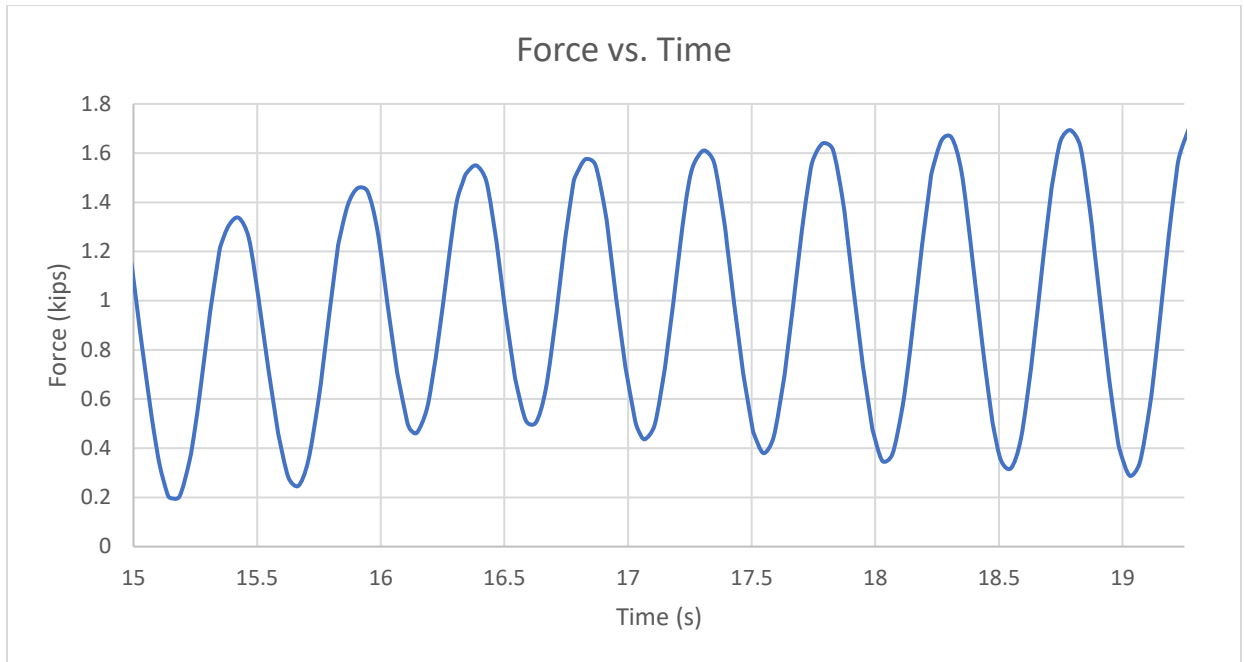


Figure 22: Force exerted on specimen 3 over time

The visual inspection of specimen 3 prior to testing showed several large, elongated voids and a minor deformity in the material near the grips. The voids, as before, can be attributed to the injection process, however, the minor deformity in the material near the grips is likely the result of an error in the cutting process when the specimen was extracted from the exterior of the crosstie. Despite the external deformities and voids, the failure of Specimen 3 originated from a large, flat void beneath the surface of the specimen, as shown in Figure 23.

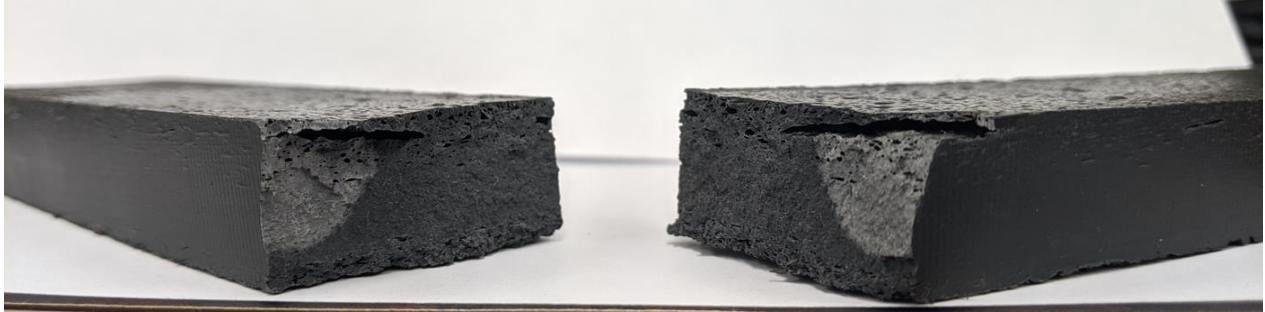


Figure 23: Specimen 3 post failure

This unseen void led to a very early failure in the specimen, which fractured 1470 cycles into the experiment. The post-mortem visual inspection showed that despite the internal origin of failure, several potential failure points and crack propagations were evident on the specimen's exterior, all originating from the aforementioned voids and defects. The cracks have been circled in red in Figure 24. Closer pictures of the propagations and their sizes can be seen in the appendices of this thesis.

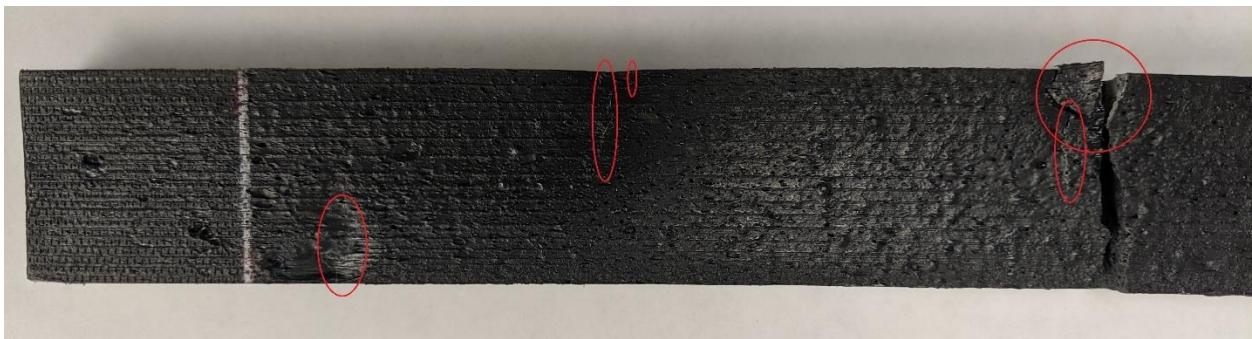


Figure 24: Crack propagation in Specimen 3

The multiple points of failure resulted in a significantly lower modulus of elasticity, as seen in Figure 25, which was measured at roughly 208,000 psi.

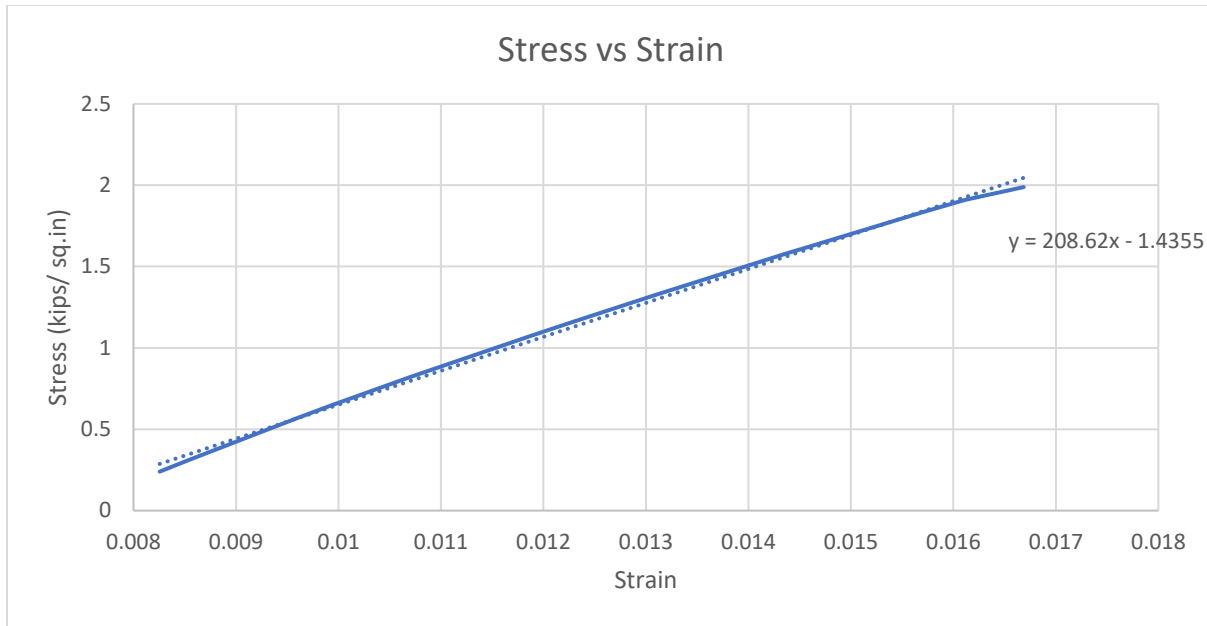


Figure 25: Stress strain relationship in Specimen 3

6.2 Complications encountered

Due to a lack of machine availability at the Structural and Materials Engineering Lab at the Center for Infrastructure Renewal, the experiments were discontinued, resulting in data collection from only three of the anticipated twenty samples. The lack of machine and personnel availability on the RELLIS campus resulted in the need to seek other testing sites.

It was determined that the most practical way to continue this research was to purchase an MTS testing frame specifically for use in the Department of Ocean Engineering's Materials and Structures lab. With this conclusion, an MTS 812.21 machine with a loading capacity of 3.3 kips (15 kN), which is pictured in Figure 26, was purchased.



Figure 26: MTS fatigue testing machine in Ocean Engineering Materials and Structural Lab

With the purchase of the new machine, the research regimen was refocused to concentrate on assembly, set up, and calibration of the machine. This included any equipment that did not come standard with the machine, such as hoses, hydraulic pump unit connections, proper pipe fittings, grips, grip adaptors, and a control system for the machinery. An attempt was made to run the machine with an MTS 407 controller, however, despite the best efforts of the research group and MTS experts, the machine could not run with the controller available, introducing a need to seek out yet another avenue for testing. Moving forward, the machine will be run using a Dewetron Data Acquisition system.

6.3 Conclusions from experimental tests

In addition to purchasing a new machine, the results obtained from the experiments conducted at the Center for Infrastructure Renewal exposed the opportunities for improvements to the testing procedure as well as the material given that all specimens failed long before reaching 1,000,000 cycles. Initially, the specimens were to undergo a CT scan every 100,000 cycles to identify crack propagation and possibly points of potential failure. However, all specimens tested fractured within the first 5000 cycles of the experiment, therefore, the samples were not subjected to the CT scans.

Based on the results of the experiments, it is evident that the procedure will need to be modified before carrying out further experimentation on the material. All factors, including specimen size, force loading, frequency of testing, and number of cycles run between inspections need to be considered when developing a new procedure.

7. COMPUTATIONAL ANALYSIS PROCEDURE

7.1 Grip induced stresses

Before testing, there was a concern that the specimen might fail at the grips during the experiment due to the stress concentrations surrounding the grips. Using ANSYS, an elastic finite element model was created to display the stresses and deformations in the specimen induced by the machine grips.

A three-dimensional part representing the specimen was created in Autodesk Fusion360. Following the creation of the specimen mesh, a part was created to mimic the grips. The two parts were input into a SolidWorks assembly, where the parts and their interaction were defined. After adding the appropriate dimensions to each part, the parts were then imported into ANSYS Work Bench, where a mesh was constructed. In ANSYS Work Bench, a new material was defined, using the material properties shown in Table 2. The newly defined material was assigned to the specimen, whereas properties for structural steel, seen in Table 3 were assigned to the grips.

	A	B	C
--	---	---	---

Table 2: Material Property Inputs for HDPE Glass Fiber Composite










3	 Density	54.4	lb ft ⁻³ 
4	 Isotropic Elasticity		
5	Derive from	Young's Modulu...	
6	Young's Modulus	2.5E+05	psi 
7	Poisson's Ratio	0.4	
8	Bulk Modulus	2.8728E+09	Pa
9	Shear Modulus	6.156E+08	Pa
10	 Tensile Yield Strength	1500	psi 
11	 Tensile Ultimate Strength	3000	psi 

Table 3: Material Properties of Steel

Properties of Outline Row 4: Structural Steel			
	A	B	C
1	Property	Value	Unit
3	Density	7850	kg m ⁻³ ▼
4	Isotropic Secant Coefficient of Thermal Expansion		
6	Isotropic Elasticity		
7	Derive from	Young's Modu... ▼	
8	Young's Modulus	2E+11	Pa ▼
9	Poisson's Ratio	0.3	
10	Bulk Modulus	1.6667E+11	Pa
11	Shear Modulus	7.6923E+10	Pa
12	Strain-Life Parameters		
20	S-N Curve	Tabular	
24	Tensile Yield Strength	2.5E+08	Pa ▼
25	Compressive Yield Strength	2.5E+08	Pa ▼

Once the appropriate material properties were assigned to their parts, the geometric parts were imported into ANSYS Mechanical, where the magnitude, direction, and location of the external forces and displacements applied to the specimen are defined. In the case of studying stresses around the grips, the top grips are defined as a rigid body with zero displacement and no external forces are applied. However, the specimen is defined as a deformable body, with a force applied on the end opposite to the grips. This force simulates the force an MTS fatigue testing frame would exert on the specimen during the experiments. A depiction of the specimen and force modeled can be seen in Figure 27. The placement of the exerted force is represented by a red arrow, indicating both the location and direction of the force.

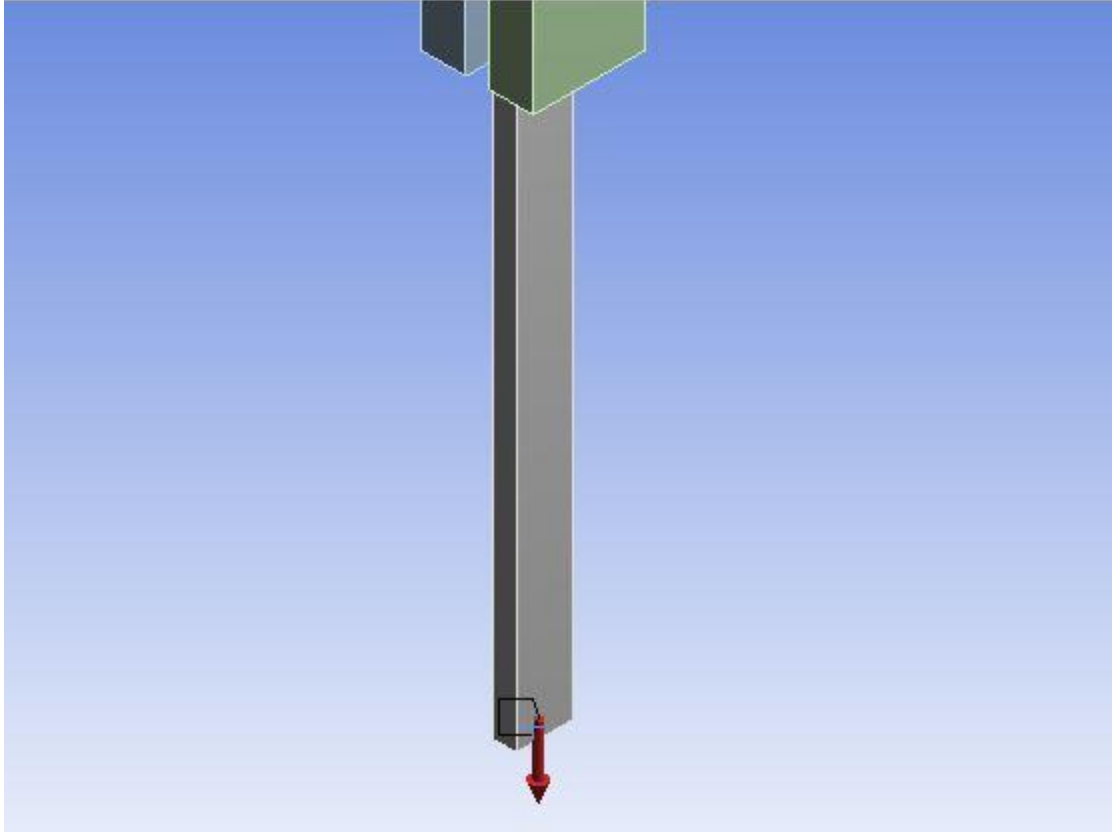


Figure 27: Force applied to the specimen for computational analysis

Similarly, there is a zero-displacement boundary condition applied at the top of the specimen, as that part of the specimen is held motionless by the grips. Next, boundary conditions defining the contact points between the grips and the specimen were defined. The contact points were defined in ANSYS Mechanical as bonded, due to the tightly gripped specimen and inability for the specimen to slip, resulting in the specimen and grip behaving as one part with differing material properties. Once the appropriate boundary conditions were applied, a mesh could be generated using ANSYS Mechanical, as shown in Figure 28.

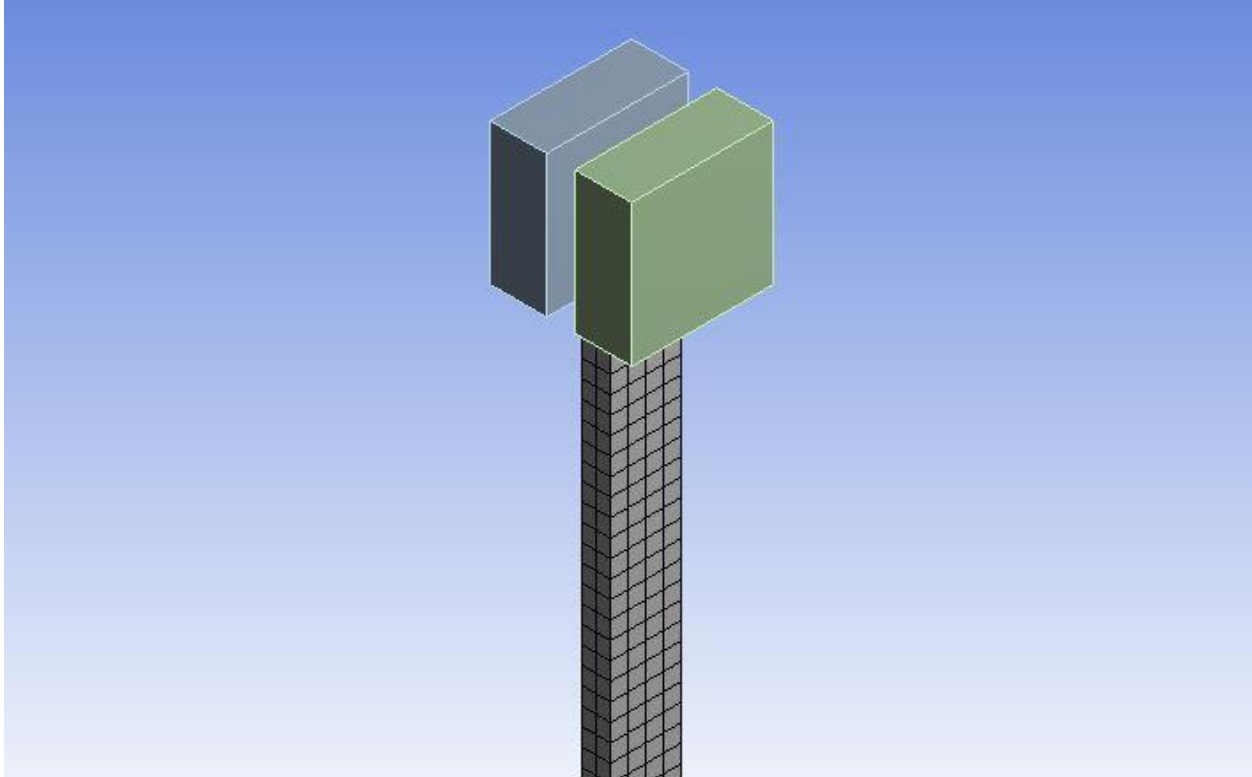


Figure 28: Mesh of the specimen

After the mesh was generated, using ANSYS Work Bench, the desired parameters to be obtained in the simulation were selected. For this experiment, the Von Mises stresses, total deformation, and equivalent elastic strain were determined.

7.2 Pore induced stresses

The analytical procedure for determining the stresses around the pores in a sample is very similar to the procedure used to analyze the stresses induced by the grips, However, the analysis of the stresses induced by pores is far more complicated and tedious from a three-dimensional modeling standpoint. HDPE glass fiber composite material has pores that vary in size, though spacing and frequency of the voids is fairly consistent throughout the porous interior of the crosstie.

In order to accurately model the stresses around the pores, numerical values for pore size, spacing between the pores, and the average number of pores in a given area were required. These values were obtained by observing a cross section of a 7 in. X 9 in. X 108 in. standard crosstie, shown in Figure 29.

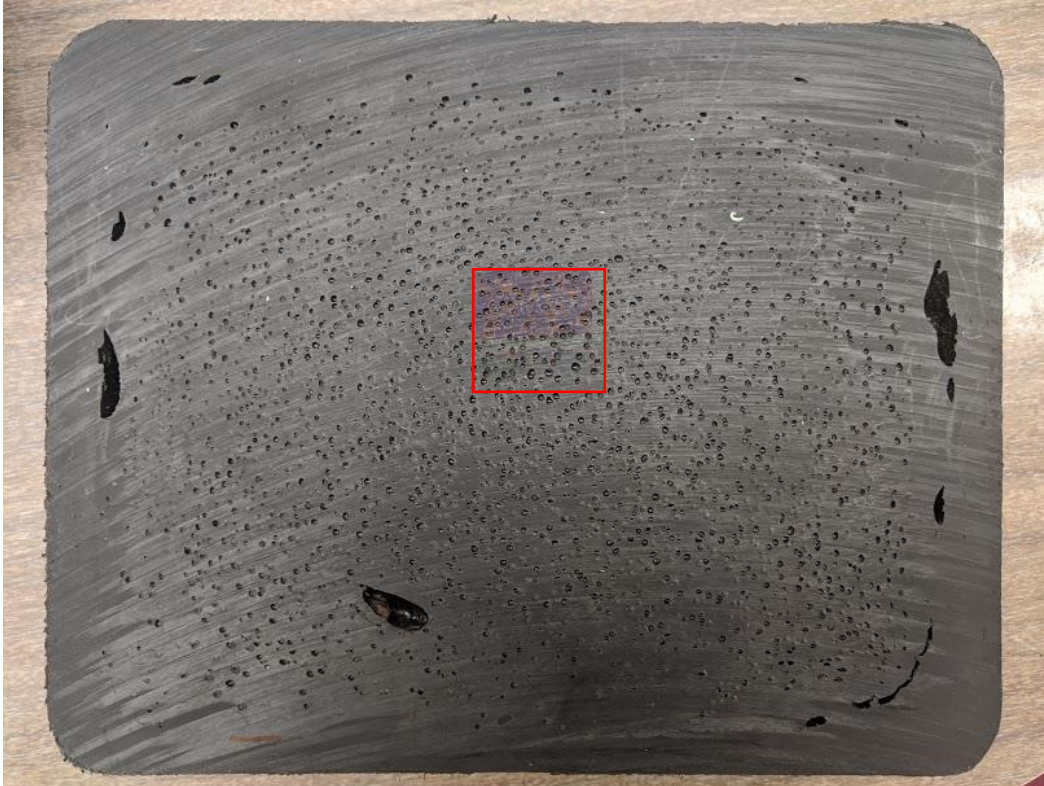


Figure 29: Cross sectional view of HDPE glass fiber composite crosstie

Also seen in Figure 29 is a red box, indicating the sample area from which the data for analysis was extracted, which is magnified in Figure 30. The red box represents a 1 in. X 1 in. section of the porous interior of the crosstie. Within the confines of the 1 in. X 1 in. area, the number of pores were counted, and marked. Using the given space, the diameter of each individual pore within the sample area was measured. The statistics for the sample can be found in Table 4.

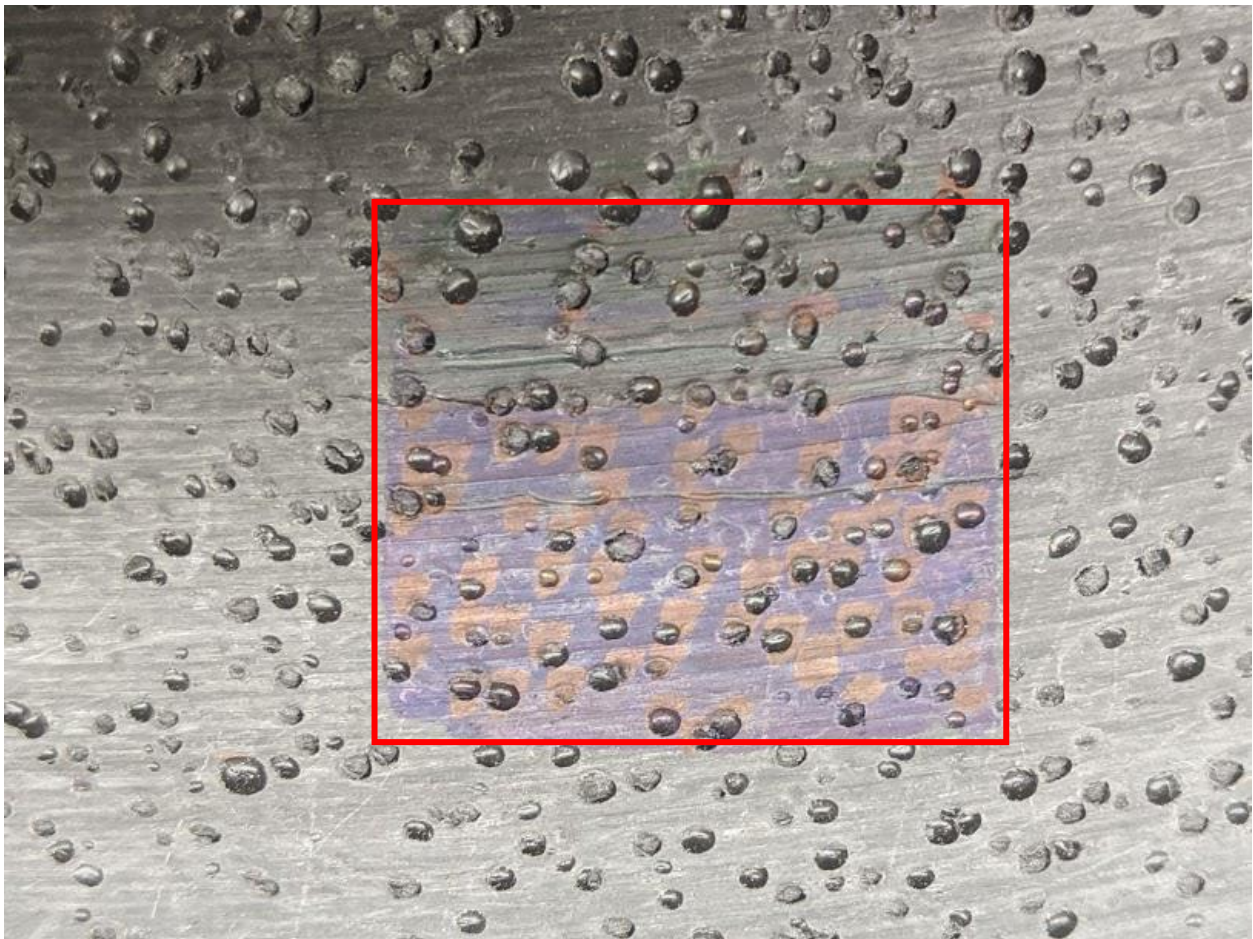


Figure 30: Sample area taken for void statistics

Table 4: Pore Statistics

Pores in 1 in. X 1 in. Area	
Average Number of Pores	101
Average Pore Size (in)	0.0547
Minimum Pore Size (in)	0.0255
Maximum Pore Size (in)	0.0890

Using the data obtained from the inspection of the pores, a three-dimensional mesh used for the finite element analysis could be created. As stated previously, due to the academic license limitations, a complete sample could not be analyzed in ANSYS. However, a small portion of the sample with accurate pore sizes, frequency and distribution could be modeled. As discussed in the literature review portion of the experimental methodology, the minimum number of voids that can be modeled and still produce an accurate averaged solution is 38. Therefore, a python code was used to generate 38 random pores, given the average, minimum and maximum pore sizes observed in the visual inspection. The 38 randomly generated pore sizes were then taken into account while constructing a three-dimensional mesh of the sample. Since the average number of pores in the 1 in. X 1 in. sample space was determined to be 101, it is evident that the 38 pores were to be placed within an area of 0.38 in. X 1 in.

Following the same procedure as before, the material was imported into ANSYS Work Bench where its material properties were defined, using the manufacturing companies' specifications previously listed. However, because only a small portion of the specimen was

being analyzed, there were no grips inserted into this analysis. Due to the lack of grips, there was an additional zero displacement boundary condition added to the top of the specimen, as it is assumed the sample being observed is taken from the center of a full-scale specimen, and there is no displacement between the specimen and the sample. A force is applied to the center of the underside of the specimen to simulate the forces exerted on the specimen by the loading frame. Once these steps were completed, a detailed finite element mesh as depicted in Figure 31 was created for the purpose of studying the potential degradation of specimen life.

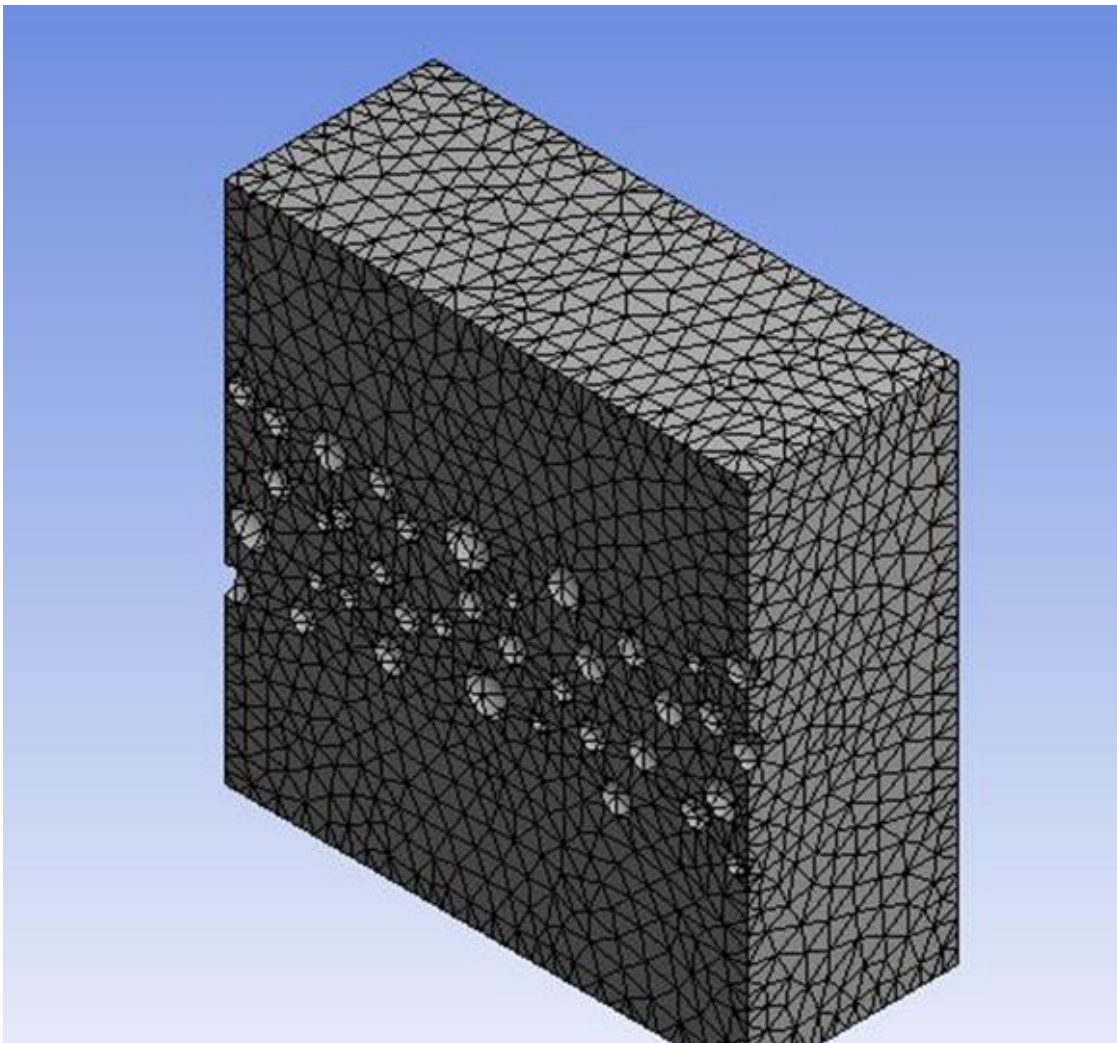


Figure 31: Mesh of porous surface

Similar to the previous stress analysis, after the mesh was generated using ANSYS Work Bench, the desired parameters to be obtained in the simulation were selected. For this experiment, the Von Mises stresses, total deformation, and equivalent elastic strain were to be determined. Once selected, the analysis was completed.

8. FINITE ELEMENT AND STRESS ANALYSIS

Following the completion of the experiments at the center for infrastructure renewal, research on the material took on an analytical shift, introducing the need for finite element analysis. The purpose of the analysis was to determine the stresses induced on the specimen by the grips and around the pores. The analysis was done using the programs ANSYS Work Bench and ANSYS Mechanical. The solutions obtained in the analysis represent the Von Mises stresses, equivalent strain, and total deformation in the material and how each varied throughout a cycle within the experiments.

8.1 Grip Analysis

One concern that was brought up prior to testing was the amount of stress induced on the specimens by the grips. Due to this concern, a computational model was constructed to study the effects of gripping on the mechanical response of the specimens. The specimens were modeled three dimensionally before being imported to ANSYS for the analysis of mechanical behaviors. The specimens in the model were created to mimic those which were used in the physical experiments. Therefore, the sample size in the three-dimensional model was 0.75 in. X 1.5 in. X 12 in., resulting in a cross-sectional area of 1.125 in^2 . and a necessary axial force of 1688 lbf. Using the ANSYS fatigue model, the stresses were obtained and animated to show how the stresses in the specimen change throughout the course of a cycle. Figures 32 and 33 show the predicted stresses induced by the grips when the specimen is at peak loading.

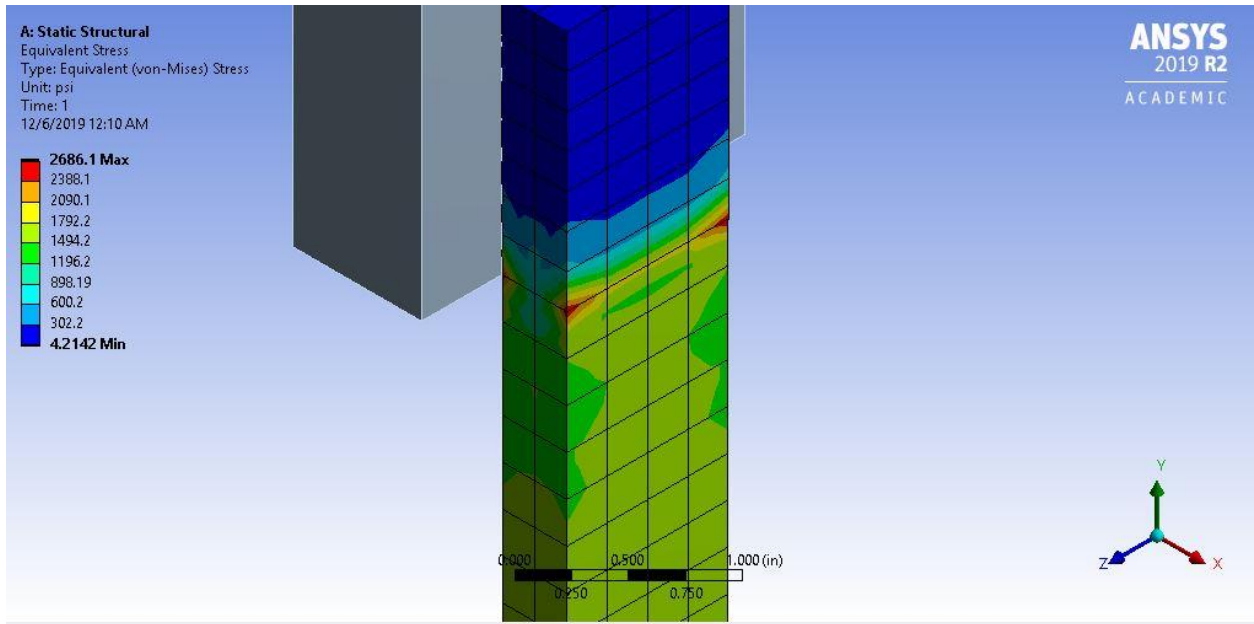


Figure 32: Stresses induced by grips

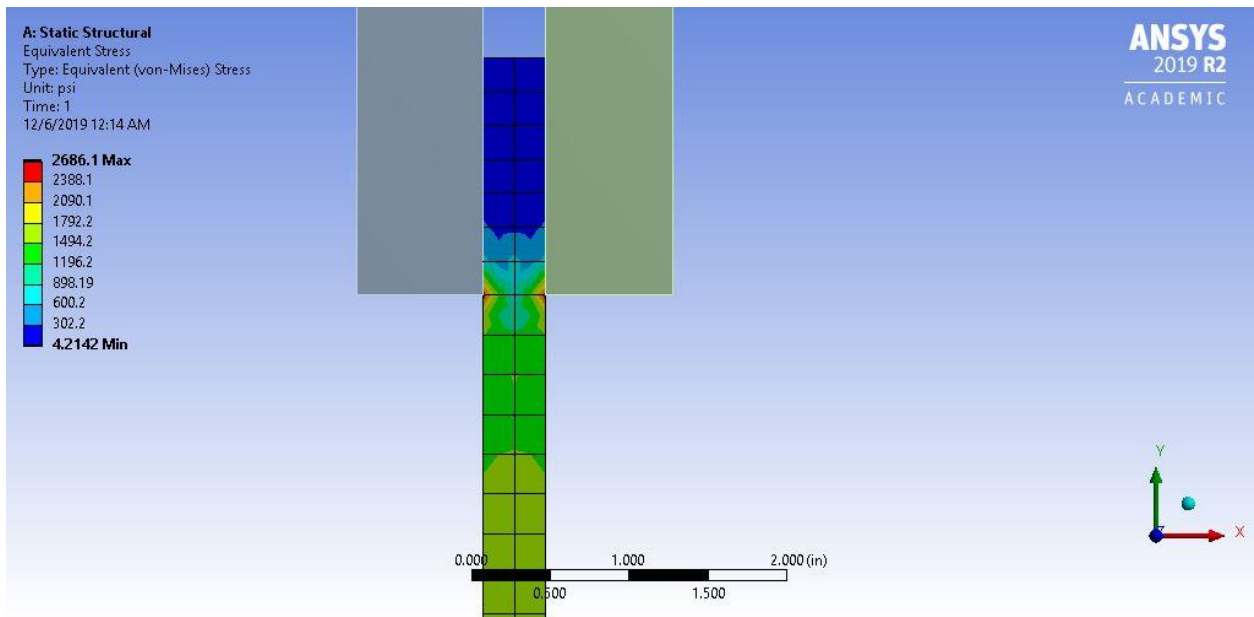


Figure 33: Stresses induced by grips

As shown in Figures 32 and 33, the predicted stresses in the specimen near the grips are substantially larger than the stresses induced elsewhere. The maximum stress in the specimen occurs at the edge of the grips with nearly 2700 psi, whereas the intended maximum stresses were roughly 1500 psi. However, throughout most of the specimen, the maximum stresses experienced during testing were 1500 psi as expected.

The strain in the specimens was also predicted with the computational model, as shown in Figure 34. The relationship between the stress and the strain seen in the specimens remain linear, as expected for an elastic stress-strain relationship with material of this nature.

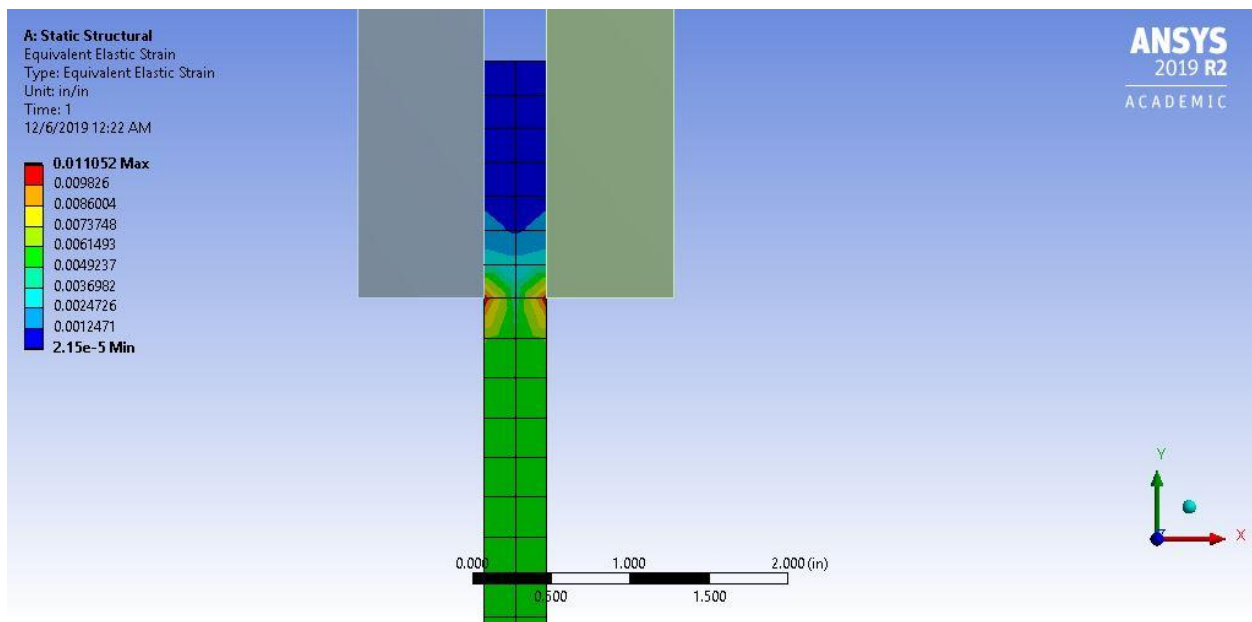


Figure 34: Equivalent elastic strain in the specimen

Lastly, the deformation experienced in the specimen do the cyclic tension force applied along the vertical axis was predicted using the computational model. It is evident in Figure 35 that the specimen deformed uniformly throughout the sample, with the largest deformation occurring at the placement of the load point. Due to the contact surface between the grips and

specimen defined as bonded, and zero displacement boundary condition, there was no displacement measured in the specimen at the grips.

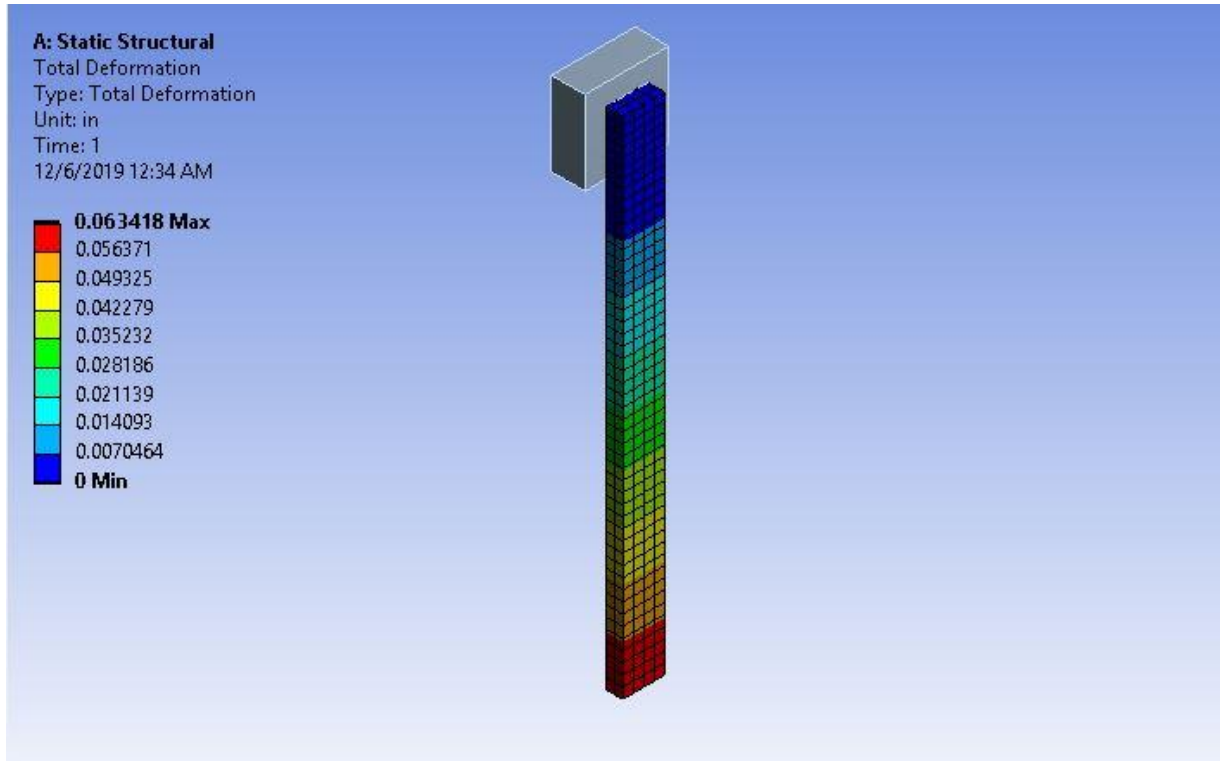


Figure 35: Total deformation in the specimen

8.2 Pore Analysis

The analysis of the mechanical response of the specimens including voids was used to focus on determining the effects of porosity on fatigue life. To begin, As stated in the procedure, the minimum number of pores allowable in modeling that produce accurate results is 38, thus, resulting in the model created for computation having 38 pores. The three-dimensional model used has dimensions of 1 in. X 1 in. X 0.75 in., with pores occupying an area of 0.38 in². Though it was discovered the samples had voids in the interior, the model studied

in this situation focuses on only the visible pores at the surface of the specimens. The stresses the specimen experienced due to the surface voids is analyzed in Figure 36.

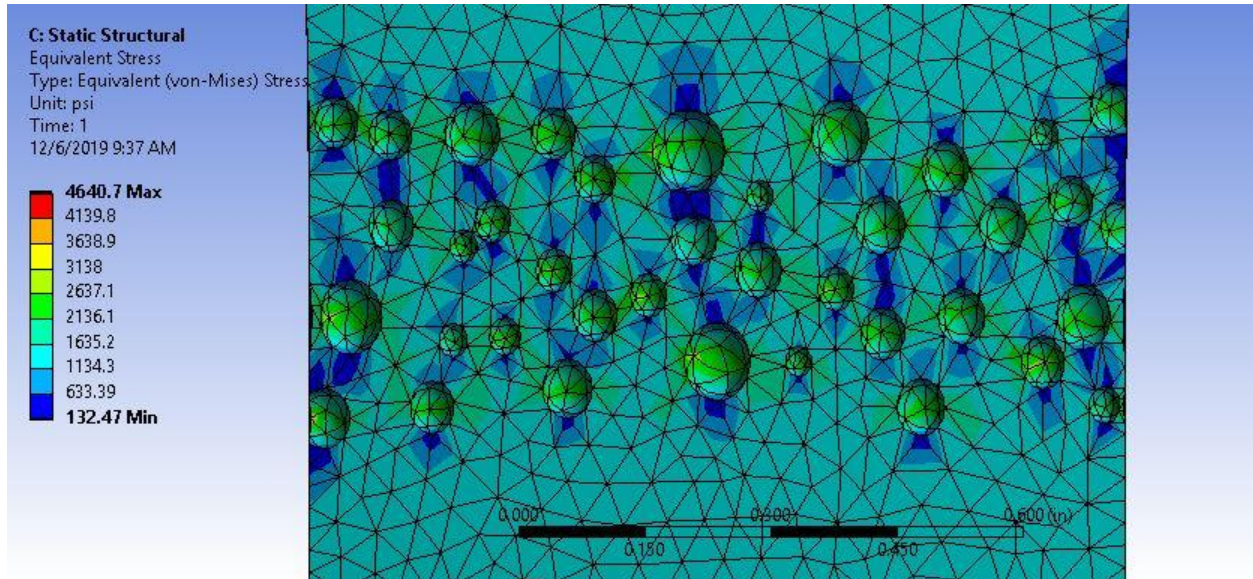


Figure 36: Stresses around the pores

As shown in Figure 33, the maximum stresses in the porous specimen are encountered in the voids, along their edges that meet the flat surface of the specimen. In addition, the maximum stress within the voids is nearly 2000 psi higher than the stresses induced by grips. This gives a reasonable explanation as to why all samples failed at voids on the surface during experimentation, while the area gripped was seemingly unaffected. The stresses were also significantly greater around the pores in the horizontal plane, normal to the direction of the forces induced by the machine, and minimal stresses occurred in the vertical direction between pores.

Similarly, the strain increased significantly when pores were introduced into the specimen model, as portrayed in Figure 37.

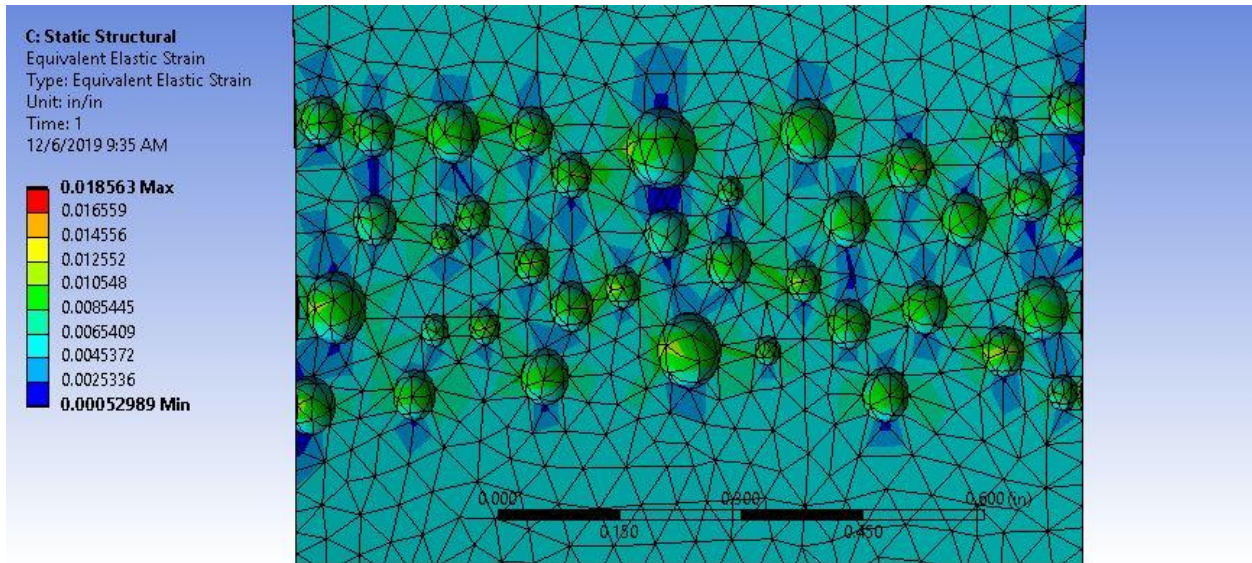


Figure 37: Elastic strain on a porous surface

Lastly, the total deformation of the specimen with a porous exterior was model and is shown in Figure 38. The face containing the pores experienced significantly more deformation than the flat face. Furthermore, it is evident that the location of the voids also plays a large role in the deformation of the material surrounding them, resulting in larger deformations in the material.

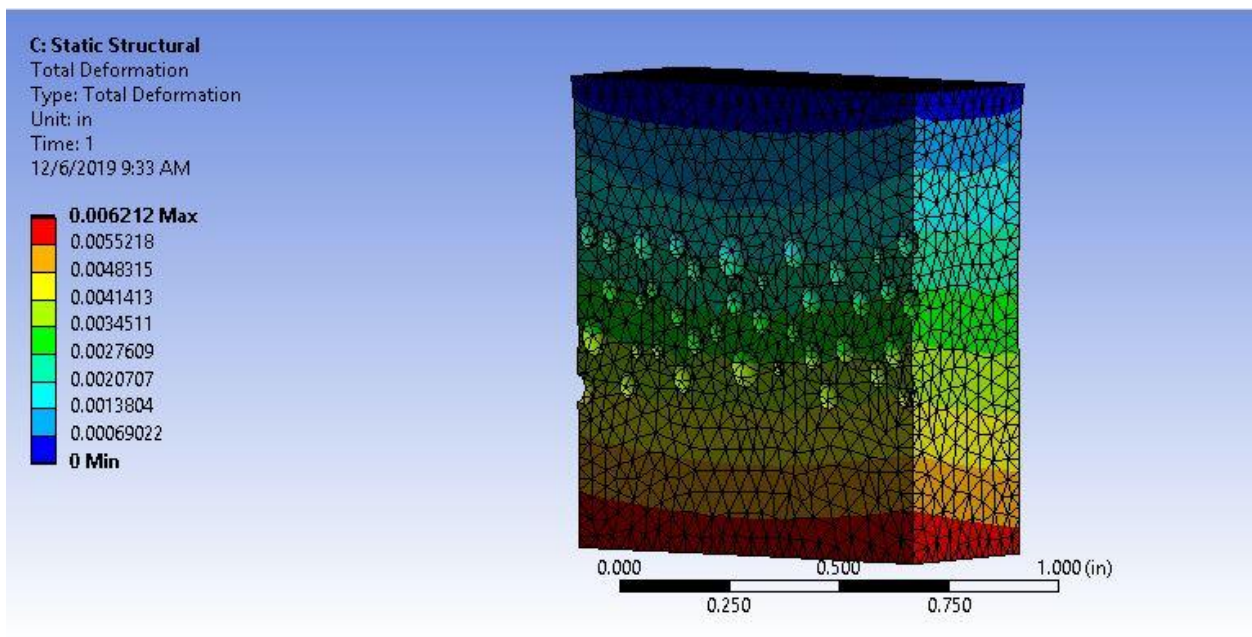


Figure 378: Deformation on a porous surface

9. RECOMMENDATIONS FOR FURTHER TESTING

There is great potential for application of this material in the field based on the experiments contained in this thesis. The initial intent of the research was to test 20 samples in cyclical fatigue to one million cycles, observing changes in the material and defect propagation 100,000 cycles. However, due to the unavailability of machinery and personnel at the testing facility, only three samples were tested experimentally. This leads to the recommendation that all further experimentation be done using the newly purchased MTS fatigue testing machinery in the Ocean Engineering Structures and Material's lab located in the Haynes Engineering Building.

In addition, the procedure is in need of modification. The most obvious contributing factor to the premature specimen failure was the presence of voids at the surface of the specimen. The voids in the specimen can be attributed to the specimen size determined before testing. The specimen cross section use in this experiment was 1.5 in. X 0.75 in. However, as is evident in Figure 39, voids due to the injection molding process extend within roughly 0.5 of the specimen surface. Therefore, for further testing, the specimens cut from the exterior portion of the crosstie should have a cross sectional area of 1 in. X 0.4 in. to avoid premature failure and produce more precise material properties. The experimental procedure of the experiment should stay the same, with the specimens being tested to one million cycles if possible. Every 100,000 cycles, the specimens should be inspected using CT scans to determine the effects of the cyclical forces on the interior of the specimen.



Figure 39: Distance from material edge to voids

In order to gain a better understanding of the material as a whole, future experimentation should also test samples taken from the porous core of the material in order to gain a better understanding of the fatigue behavior of the material. A comparison of the solid and porous materials fatigue life and experimentally calculated properties should be taken into consideration.

10. CONCLUSION

In conclusion, the recycled HDPE glass fiber composite material has promising applications in use for structures like railroad crossties, construction mats, piers, sea walls and more, as its material properties are superior to those of its competing counterparts. The polymer composite's resilience to water and high modulus of elasticity makes it perfect for use in coastal environments.

However, following the conclusion of the experimental analysis, a recommendation regarding the manufacturing of the material should be made. The voids experienced in the interior portion of the material proved to be detrimental to the fatigue life of the specimens, leading to the conclusion that the number of voids should be decreased, and the distance of voids from the surface of the crosstie should be increased to increase the fatigue life of the material and protect against potential unexpected failure.

Following the experiments presented in this thesis, it is highly recommended that further experimentation should be done following the procedure discussed in the recommendations portion of the thesis.

REFERENCES

1. ANSYS. Inc. (2004). ANSYS Contact Technology Guide.
2. Bolin, Christopher A., and Stephen T. Smith. "Life Cycle Assessment of Creosote-Treated Wooden Railroad Crossties in the US with Comparisons to Concrete and Plastic Composite Railroad Crossties." *Journal of Transportation Technologies*, vol. 03, no. 02, 2013, pp. 149–161., doi:10.4236/jtts.2013.32015.
3. Boresi, A. P. and Schmidt, R. J. and Sidebottom, O. M., 1993, ***Advanced mechanics of materials***, John Wiley and Sons, New York
4. Burgers, Travis, and Jenő Balogh. "EFFECTS OF ENVIRONMENTAL EXPOSURE ON TIMBER RAILROAD BRIDGE/TRACK MEMBERS AND CONNECTORS." *Penn State Doctorate Dissertation*, Dec. 2004.
5. FEMA "Material Durability in Coastal Environments," Coastal Construction Manual Resources, Published 2012
6. Harper, Charles A. (2002). *Handbook of Plastics, Elastomers, and Composites (4th ed.)*. McGraw-Hill. ISBN 0-07-138476-6.
7. Hay, William Walter (1982). *Railroad Engineering*. Wiley. ISBN 0-471-36400-2.
8. Helms, K.L.E. "Modeling of Damage Evolution at Grain Boundaries in Polycrystalline Solids," Texas A&M University, August, 2000
9. Hetényi Miklós Imre. *Beams on Elastic Foundation: Theory with Applications in the Fields of Civil and Mechanical Engineering*. Univ. of Michigan Pr., 1976.

10. Huang R, Xu X, Lee S, Zhang Y, Kim BJ, Wu Q. High Density Polyethylene Composites Reinforced with Hybrid Inorganic Fillers: Morphology, Mechanical and Thermal Expansion Performance. *Materials (Basel)*. 2013;6(9):4122–4138. Published 2013 Sep 17.
11. Manalo, A., et al. “A Review of Alternative Materials for Replacing Existing Timber Sleepers.” *Composite Structures*, vol. 92, no. 3, 2010, pp. 603–611., doi:10.1016/j.compstruct.2009.08.046.
12. Owen, Toni. “What Are the Dangers of Treated Railroad Ties?” *Hunker*, Hunker.com, 23 Aug. 2018, www.hunker.com/13405931/what-are-the-dangers-of-treated-railroad-ties.
13. Rodrigues, P. “Quantifying Normal Stresses in Composite Crossties,” Texas A&M University, September, 2019
14. Soudki, Khaled A., et al. “Closure to ‘Performance of Bridge Timber Ties under Static and Fatigue Loading’ by Khaled A. Soudki, Sami H. Rizkalla, and A. Shakoor Uppal.” *Journal of Bridge Engineering*, vol. 6, no. 4, 2001, pp. 295–295., doi:10.1061/(asce)1084-0702(2001)6:4(295.2).
15. Stacey, Barbara. “Questions About the Railway Tie Association.” *Railway Tie Association*, Railway Tie Association, 2018, www.rta.org/faqs-main.
16. Stagl, Jeff. “Rail Insider-Class I Railroads Continue the Longer-Train Trend. Information For Rail Career Professionals From Progressive Railroading Magazine.” *Progressive Railroading*, BNSF, July 2018, www.progressiverailroading.com/bnsf_railway/article/Class-I-railroads-continue-the-longer-train-trend--55035.